Int. J. Fuzzy Syst. (2025) 27(6):1904–1923
https://doi.org/10.1007/s40815-024-01880-3

Master–Slave Synchronization for Fuzzy Markovian Jump Complex Dynamical Networks with Coupling Delay Via Fault-Tolerant Control

G. Brundhashree[1] · Saravanan Shanmugam[2] · S. Magudeeswaran[3] · R. Vadivel[4] · Nallappan Gunasekaran[5] · Mohamed Rhaima[6]

Received: 3 June 2024 / Revised: 24 August 2024 / Accepted: 23 September 2024 / Published online: 21 November 2024

Abstract This study addresses the challenge of synchronizing master and slave systems in complex dynamic networks using Takagi-Sugeno (T-S) fuzzy Markovian jump models, with the presence of coupling delays. To enhance synchronization robustness, fault-tolerant control mechanisms are implemented. State feedback controller is converted to fault-tolerant control and control gain matrices are derived to improve system stability in the presence of faults. Using Lyapunov-krasovskii functional and Linear Matrix Inequalities (LMIs), this study establishes precise stability proofs and analytical constraints to ensure stochastic mean-square stability. The use of LMIs enables the systematic design of fault-tolerant controllers and provides a formal framework for handling faults while maintaining system performance. Moreover, numerical simulations using a MATLAB LMI toolbox validate the effectiveness of the proposed fault-tolerant control strategy under various fault scenarios, highlighting its practical applicability in complex dynamical networks.

Keywords Complex dynamical networks · Fault-tolerant control · Lyapunov-Krasovskii functional · Synchronization · Takagi-Sugeno fuzzy

✉ Saravanan Shanmugam
saravanantvu@gmail.com

✉ R. Vadivel
vadivelsr@yahoo.com

Nallappan Gunasekaran
gunasmaths@gmail.com

Mohamed Rhaima
mrhaima.c@ksu.edu.sa

1 Department of Mathematics, Gobi Arts and Science College, Gobichettipalayam, Tamil Nadu 638453, India

2 Center for Computational Biology, Easwari Engineering College, Chennai, Tamil Nadu 600089, India

3 Department of Mathematics, Sree Saraswathi Thyagaraja College, Pollachi, Tamil Nadu 642107, India

4 Department of Mathematics, Faculty of Science and Technology, Phuket Rajabhat University, Phuket 83000, Thailand

5 Eastern Michigan Joint College of Engineering, Beibu Gulf University, Qinzhou 535011, China

6 Department of Statistics and Operations Research, College of Sciences, King Saud University, Riyadh 11451, Saudi Arabia

1 Introduction

Complex dynamical networks (CDNs) are found in various systems, extending from the World Wide Web and electric grids to biological systems and transport networks. These networks consist of interconnected nodes that exhibit a range of collective behaviors such as fluttering, consensus, and self-organization. In recent years, CDNs have been increasing attention toward understanding the structural, dynamical properties and their implications in real-world applications. Over the past three decades, researchers have extensively investigated CDNs, the cluster synchronization in CDNs, the phenomenon of almost periodic solutions in CDNs, robustness and stability of CDNs, pinning control strategies for stabilizing CDNs, highlighting its importance in achieving functional coherence in complex systems domains [1–3]. Authors [4–6] investigated in the robustness and synchronization properties of CDNs, elucidating the resilience of these networks against perturbations and their ability to achieve coordinated behavior among constituent nodes and in tracking control algorithms for CDNs, offering practical methods for regulating the trajectories of network dynamics toward specified targets.

Synchronization, a widespread phenomenon in CDNs, is about harmonizing multiple components or processes so that they function smoothly, ensuring optimal and coherent performance. This concept is of great importance in various fields, such as regulating the human heartbeat, ensuring secure communication channels, advancing information science, and improving image processing techniques. The importance of the concept also extends to complex networks as it has diverse applications in various fields such as ecosystems, technology, communication security, seismology, and parallel image processing. Synchronization has attracted much attention in the literature due to its fundamental role in improving the efficiency and reliability of networked systems. Authors investigated in [7] explored the interconnectedness between synchronization and network links, shedding light on its intricate dynamics within complex infrastructures. Authors investigated in [8] contributed to the discourse by investigating the static aspects of synchronization, providing valuable insights into its stability and robustness characteristics. Additionally, [9] investigates the application of synchronization in parallel image processing, offering practical methodologies for synchronization principles to optimize computational tasks.

In the search for synchronization in complex networks, scientists have encountered significant challenges, especially with respect to the dynamic nature of network topologies. The topological connections in these networks can be subject to random mutations in response to complex environmental factors, posing formidable obstacles to efforts to control synchronization. To overcome these challenges, researchers have used the Markov process as a valuable tool for modeling sudden topological changes. This approach has led to a proliferation of studies focusing on synchronization control in Markov jump complex dynamic networks (MJCDNs). Through the lens of MJCDNs, researchers aim to elucidate the intricate dynamics of synchronization in the presence of dynamic network structures [10]. The literature reflects a growing body of research dedicated to synchronization control in MJCDNs. Authors have contributed significantly to this field, exploring diverse methodologies and theoretical frameworks for managing synchronization amidst dynamic network topologies [11–13]. However, challenges persist, prompting researchers to explore innovative approaches to synchronization control. Authors have studied in nonlinear control methods, offering insights into their applicability in managing synchronization within evolving network structures [14]. Additionally, [15] investigated observer-based techniques, shedding light on their potential to address synchronization control challenges in complex network environments.

The T-S fuzzy model stands out as assessing contemporary control systems. This model offers a unique framework for representing nonlinear systems within a linear framework, employing fuzzy membership functions and IF-THEN fuzzy rules in [16,17]. By advantage of these components, the T-S fuzzy model simplifies defuzzification, allowing for the application of various linear system theories to analyze nonlinear dynamical systems effectively. In recent years, scholars have increasingly recognized the applicability of T-S fuzzy models in addressing stabilization and synchronization challenges within complex dynamical networks. This recognition has spurred the development of numerous fuzzy control methods tailored to the intricacies of these networks [18–21] CDNs, as a distinct category within nonlinear systems, present unique modeling and control challenges. However, T-S fuzzy models offer a promising approach to address these challenges, enabling the effective representation of CDNs within a structured framework. While the literature reflects a growing interest in applying T-S fuzzy models to complex networks, there remains a need for further research to explore and refine fuzzy control methods tailored to the specific characteristics of these networks. Author studies have contributed in [22], focusing on synchronization challenges within complex networks and proposing fuzzy control strategies.

In real-world physical systems, prolonged operation often leads to component degradation or damage, especially in critical elements such as actuators and sensors. Consequently, addressing fault-tolerant control (FTC) becomes crucial in both system design and operation. Researchers have extensively explored FTC strategies across a variety of systems and objects in [23]. Fault-tolerant attitude control has two approaches, namely active FTC and passive FTC. These methodologies have undergone significant research scrutiny over the past few decades. Studies have focused on various methodologies, including adaptive control [24], performance control [25], and intelligent control [26]. In the realm of fault-tolerant attitude control, actuator faults are a significant concern. Active fault-tolerant attitude control strategies aim to modify these faults by considering fault estimation errors and control input constraints. These strategies are essential for ensuring the continued operation and stability of systems despite the presence of faults [27].

In recent years, there have been notable research works focusing on delay-dependent synchronization criteria for MJCDNs, particularly utilizing a T-S fuzzy approach. Scholars have investigated the integration of various tools such as fuzzy controllers, Lyapunov-Krasovskii functional (LKF), and numerical simulations to investigate this area [28]. Additionally, recent studies have delved into the analysis of nonfragile synchronization control problems in discrete-time Takagi-Sugeno fuzzy MJCDNs. These investigations have employed fuzzy-basis-dependent and mode-dependent Lyapunov functions, shedding light on novel methodologies for addressing synchronization challenges [29]. However, despite advancements in synchronization control, existing fault-tolerant control methods often fall short of compre-

hensively addressing real-world conditions. Consequently, there is a growing interest in integrating T-S fuzzy synchronization into fault-tolerant control schemes, particularly within the context of CDNs. This innovative approach not only offers a novel perspective but also serves as a motivation for further exploration and research in this area. By integrating T-S fuzzy synchronization into FTC schemes for CDNs, researchers aim to develop robust and adaptive control strategies capable of addressing real-world challenges such as component degradation and system faults. This integrated approach leverages the flexibility and adaptability of fuzzy logic to enhance the fault tolerance and resilience of CDNs, ultimately improving their reliability and performance in dynamic operating environments. The authors in [30] introduce a stability method for nonlinear processes, while [31] enhance robustness using observer-based control in singular Takagi-Sugeno systems. In [32], apply model-based fuzzy control to networked systems, addressing challenges like time delays. Additionally, in [33], survey highlights the broad applicability of fuzzy control in mechatronics, emphasizing its role in managing nonlinearities and uncertainties. Collectively, these works demonstrate the adaptability and effectiveness of fuzzy control in various complex systems. Based on the insights from the literature, this article focuses on the FTC of MJCDNs within a specific class of T-S fuzzy systems with input constraints. The key contributions of this study are as follows:

- The study addresses the synchronization problem for MJCDNs modeled using the T-S fuzzy framework, accounting for coupling delays.
- By employing the Kronecker product in combination with novel integral inequalities and delay-dependent conditions, the paper ensures stochastic synchronization in the mean-square sense for the T-S fuzzy MJCDNs through an innovative LKF approach.
- A fault-tolerant controller is designed to effectively synchronize the MJCDNs, ensuring resilience against potential faults within the system. The control gain matrix of the closed-loop system is derived using LMI techniques, providing a robust framework for system stability.
- Finally, numerical examples validate the theoretical findings, demonstrating that the synchronization criteria are not only theoretically sound but also practical for real-world applications, as illustrated by the second example provided.

Notations The notations used in this paper are quite and fairly standard. Throughout this paper, $\mathbb{R}$ is the set of all real numbers, $\mathbb{R}^n$ is the n-dimensional Euclidean space, $\mathbb{R}^{n\times n}$ denotes the set of all $n\times n$ real matrices. ($diag\{\ldots\}$ denotes a diagonal matrix. $P>0$ ($P\geq 0$) means that matrix P is a real symmetric positive definite matrix (positive semi-definite). P^T represents the transpose of matrix P. Given a complete probability space(Ω, $\mathcal{F}$, $\mathcal{P}$), where Ω is the sample space, $\mathcal{F}$ is the algebra of events, and $\mathcal{P}$ is the probability measure defined on $\mathcal{F}$. The notation $A\otimes B$ stands for the Kronecker product of matrices A and B. $||\cdot||$ stands for the Euclidean vector norm. $\mathcal{E}$ stands for the mathematical expectation.

2 Problem Formulation and Preliminaries

Consider the following T-S fuzzy MJCDNs as described in references [27–29]. These networks consist of m distinct plant rules, where each rule includes N interconnected nodes. Each node represents a dynamical system with n dimensions. Plant rule ℓ: IF $\chi_1(t)$ is $\omega_{1\ell}$, $\chi_2(t)$ is $\omega_{2\ell}$, ..., $\chi_\rho(t)$ is $\omega_{\rho\ell}$, THEN

$$\begin{aligned}\dot{x}_i(t) &= R_\ell(\tau(t))x_i(t) + C_\ell(\tau(t))\tilde{g}(x_i(t))\\ &\quad + \kappa\sum_{j=1}^{N}\tilde{\Lambda}_\ell(\tau(t))\tilde{D}_{\ell ij}(\tau(t))x_j(t-\alpha(t))\\ &\quad + W_\ell(\tau(t))u_i(t),\\ x_i(t) &= \xi_i(t), \forall t\in[-\alpha,0],\end{aligned}\tag{1}$$

where $\chi(t)=[\chi_1(t),\chi_2(t),\ldots,\chi_\rho(t)]$ are the premise variables, ℓ is the number of IF-THEN rules, $\ell=1,2,\ldots,m$. $\omega_{\ell 1},\omega_{\ell 2},\cdots,\omega_{\ell\rho}$ are fuzzy sets, $x_i(t)=[x_{i1}^T(t),x_{i2}^T(t),\ldots,x_{in}^T(t)]^T\in\mathbb{R}^n$ $(i=1,2,\ldots,N)$ is the state of ith node, $\xi_i(t)$ is the continuous initial condition of the ith node, $\tilde{g}(x_i(t))$ represents a vector-valued nonlinear function, $u_i(t)$ represents the control input. $R_\ell(\tau(t))$, $C_\ell(\tau(t))$, and $W_\ell(\tau(t))$ represent the constant matrices with real values of suitable dimensions, $\tilde{\Lambda}_\ell(\tau(t))$ and $\tilde{D}_{\ell ij}(\tau(t))$ indicate the system's outer coupling configuration matrix and inner coupling configuration matrix, respectively. $\kappa>0$ is the coupling strength, $\alpha(t)$ represents the time-varying input delay satisfying $0\leq\alpha(t)\leq\alpha$ and $\dot{\alpha}(t)\leq\lambda$, where $\alpha>0$ and λ are known constants.

Consider $\tau(t)$, $t\geq 0$, represent a continuous-time Markov process characterized by continuous trajectories and assuming values from a finite set $\mathcal{F}=1,2,\ldots,\mathcal{N}$. Additionally, the transition probabilities are specified as follows:

$$Pr\{\tau(t+\Xi)=q|\tau(t)=p\} = \begin{cases}\pi_{pq}\Xi t+o(\Xi t) & p\neq q,\\ 1+\pi_{pp}\Xi t+o(\Xi t) & p=q,\end{cases}$$

in which $\Xi t>0$, $\lim_{\Xi t\to 0}(o(\Xi t)/\Xi t)=0$, and π_{pq} denotes the transition rates between the modes from p at time t to q at time $t+\Xi t$ this condition ensures that $\pi_{pq}\geq 0, \forall p\neq q, \sum_{q=1}^{N}\pi_{pq}=0, \forall p\in\mathcal{F}$.

Let $s(t)$ represent the state of the isolated node defined as

Plant rule ℓ: IF $\chi_1(t)$ is $\omega_{1\ell}$, $\chi_2(t)$ is $\omega_{2\ell}$, ..., $\chi_\rho(t)$ is $\omega_{\rho\ell}$, THEN

$$\dot{s}(t) = R_\ell(\tau(t))s(t) + C_\ell(\tau(t))\tilde{g}(s(t)). \tag{2}$$

The defuzzified fuzzy system (1) and (2) can be expressed through the fuzzy inference method as follows:

$$\begin{aligned}\dot{x}_i(t) = \sum_{\ell=1}^{m} \psi_\ell(\omega(t))\Big\{ & R_\ell(\tau(t))x_i(t) + C_\ell(\tau(t))\tilde{g}(x_i(t)) \\ & + \kappa \sum_{j=1}^{N} \tilde{\Lambda}_\ell(\tau(t))\tilde{D}_{\ell ij}(\tau(t))x_j(t-\alpha(t)) \\ & + W_\ell(\tau(t))u_i(t)\Big\}, \end{aligned} \tag{3}$$

$$\dot{s}(t) = \sum_{\ell=1}^{m} \psi_\ell(\omega(t))\Big\{ R_\ell(\tau(t))s(t) + C_\ell(\tau(t))\tilde{g}(s(t))\Big\}, \tag{4}$$

The membership function is defined as

$$\psi_\ell(\omega(t)) = \frac{\hat{\sigma}_\ell(\omega(t))}{\sum_{\ell=1}^{m} \hat{\sigma}_\ell(\omega(t))},$$
$$\hat{\sigma}_\ell(\omega(t)) = \prod_{a=1}^{\rho} \bar{\sigma}(\omega_a(t)),$$

where $\bar{\sigma}(\cdot)$ is grade of membership function.

The ith rule of T-S fuzzy node and the target node, the state synchronization error is expressed as follows:

$$\begin{aligned}\dot{e}_i(t) = \sum_{\ell=1}^{m} \psi_\ell(\omega(t))\Big\{ & R_\ell(\tau(t))e_i(t) + C_\ell(\tau(t))\hat{g}(e_i(t)) \\ & + \kappa \sum_{j=1}^{N} \tilde{\Lambda}_\ell(\tau(t))\tilde{D}_{\ell ij}(\tau(t))e_j(t-\alpha(t)) \\ & + W_\ell(\tau(t))u_i(t)\Big\}, \end{aligned} \tag{5}$$

where $e_i(t) = x_i(t) - s(t)$ and given dynamics are $e_i(t) = [e_{i1}(t), e_{i2}(t), \ldots, e_{in}(t)]^T$, and $\hat{g}(e_i(t)) = \tilde{g}(x_i(t)) - \tilde{g}(s(t))$. For simplicity, let us denote the Markov process $\tau(t)$ as p. Consequently, the provided system (5) can be expressed as

$$\begin{aligned}\dot{e}_i(t) = \sum_{\ell=1}^{m} \psi_\ell(\omega(t))\Big\{ & R_{\ell p}e_i(t) + C_{\ell p}\hat{g}(e_i(t)) \\ & + \kappa \sum_{j=1}^{N} \tilde{\Lambda}_{\ell p}\tilde{D}_{\ell ijp}(e_j(t-\alpha(t))) \\ & + W_{\ell p}u_i(t)\Big\}. \end{aligned} \tag{6}$$

The main objective of this paper is to apply fault-tolerant control to the system (6) as follows:

Now, we consider the following actuator failure model, for the control input $u_i(t)$, we denote $u_f(t)$ to describe the signal sent from the actuator discussed in [34]. It is given as follows:

$$u_f(t) = \sum_{v=1}^{m} \psi_v(\omega(t))\mathfrak{F}_{ivp}(u_i(t)), \tag{7}$$

where

$$\mathfrak{F}_{ivp} = diag\{g_{ivp}^1,\ g_{ivp}^2,\ \ldots,\ g_{ivp}^n\}. \tag{8}$$

The function matrix for actuator faults is defined as $0 \le g_{ivp-}^r \le g_{ivp}^r \le g_{ivp+}^r \le 1$, where $(r = 1, 2, \ldots, n)$, and real constants are known as g_{ivp-}^r and g_{ivp+}^r characterizing the permissible failures of the rth actuator. Additionally, $g_{ivp-}^r = g_{iv-}^r(\tau(t))$ and $g_{ivp+}^r = g_{iv+}^r(\tau(t))$ are constant matrices. By setting

$$g_{0ivp}^r = \frac{g_{ivp-}^r + g_{ivp+}^r}{2}, \quad l_{ivp}^r = \frac{g_{ivp}^r - g_{0ivp}^r}{g_{0ivp}^r},$$
$$\mathfrak{h}_{ivp}^r = \frac{g_{ivp+}^r - g_{0ivp-}^r}{g_{ivp+}^r + g_{ivp-}^r},$$

then, it is clear that,

$$\mathfrak{F}_{ivp} = \mathfrak{F}_{0ivp}(I + L_{ivp}), \quad |L_{ivp}| \le H_{ivp} \le I,$$

where

$$\mathfrak{F}_{0vp} = diag\{g_{0ivp}^1,\ g_{0ivp}^2,\ \ldots,\ g_{0ivp}^n\},$$
$$|L_{ivp}| = diag\{|l_{ivp}^1|,\ |l_{ivp}^2|,\ \ldots,\ |l_{ivp}^n|\},$$
$$\mathfrak{h}_{ivp} = diag\{\mathfrak{h}_{ivp}^1,\ \mathfrak{h}_{ivp}^2,\ \ldots,\ \mathfrak{h}_{ivp}^n\},$$

In this paper, we are interested in designing a state feedback controller of the form,

Control Rule v: IF $\chi_1(t)$ is ω_{1v}, $\chi_2(t)$ is ω_{2v}, ..., $\chi_\rho(t)$ is $\omega_{\rho v}$,
THEN

$$u_i(t) = K_{vp}(e_i(t)),$$
$$(v = 1, 2, \ldots, m) \quad \&(i = 1, 2, \ldots, N), \tag{9}$$

where K_{vp} represents the controller gain matrices to be designed. Furthermore, the reformulation of the defuzzified state feedback controller can be expressed as

$$u_i(t) = \sum_{v=1}^{m} \psi_v(\omega(t))K_{vp}(e_i(t)), \quad i = 1, 2, \ldots, N. \tag{10}$$

substituting (10) into (6), the properties of the Kronecker product are applied to derive in the following form of the closed-loop system:

$$\begin{aligned}\dot{e}(t) = \sum_{\ell=1}^{m}\psi_\ell(\omega(t))\sum_{v=1}^{m}\psi_v(\omega(t))\Big\{&(I_N\otimes R_{\ell p})e(t)\\ &+(I_N\otimes C_{\ell p})\hat{g}(e(t))\\ &+\kappa(\tilde{\Lambda}_{\ell p}\otimes\tilde{D}_{\ell p})e(t-\alpha(t))\\ &+(I_N\otimes W_{\ell p})\mathfrak{F}_{0p}(I+L_p)K_{vp}e(t)\Big\},\end{aligned}\tag{11}$$

where

$$\begin{aligned}L_p &= diag\{L_{1p},\ L_{2p},\ \ldots,\ L_{Np}\},\\ H_p &= diag\{H_{1p},\ H_{2p},\ \ldots,\ H_{Np}\},\\ K_{vp} &= diag\{K_{1vp},\ K_{2vp},\ \ldots,\ K_{Nvp}\},\\ \mathfrak{F}_{0p} &= diag\{\mathfrak{F}_{01vp},\ \mathfrak{F}_{02vp},\ \ldots,\ \mathfrak{F}_{0Nvp}\},\end{aligned}$$

$$e(t)=\begin{bmatrix}e_1(t)\\ e_2(t)\\ \cdot\\ \cdot\\ \cdot\\ e_N(t)\end{bmatrix},\quad \hat{g}(e(t))=\begin{bmatrix}\hat{g}(e_1(t))\\ \hat{g}(e_2(t))\\ \cdot\\ \cdot\\ \cdot\\ \hat{g}(e_N(t))\end{bmatrix}.$$

The purpose of this work is to frame a fault-tolerant control mechanism to attain synchronization among both systems (3) and (4). Consequently, the primary outcomes are derived in system (11), ensuring stochastic mean-square stability. Furthermore, the following beneficial definitions and lemmas are presented, which will help further analyze the main findings:

Definition 1 [35] The CDNs (1) are said to be stochastically synchronous, if synchronization error system (11) is stochastically mean-square stable, that is, for any initial conditions $(e(0), \tau(0))$, there exists a constant scalar $\mathcal{E}(e(0), \tau(0)) > 0$ such that the following condition holds:

$$\varrho\left\{\int_0^\infty e^T(t)e(t)\mathrm{d}t\,|e(0),\tau(0)\right\}\le\mathcal{E}(e(0),\tau(0)).\tag{12}$$

Remark 1 The stochastic stability of synchronization error system with Markov jump in Definition 1 means that the trajectories of the state $e_i(t)$ along the Markov process from the initial state $(e(0), \tau(0))$, converge asymptotically to the origin in the mean-square stable.

Assumption 1 [36] $\hat{g}:\mathbb{R}^n\to\mathbb{R}^n$ is a continuous vector-valued function and satisfies a sector-bounded condition which is described as follows:

$$\begin{aligned}&\left[\hat{g}(x)-\hat{g}(y)-\mathcal{G}(x-y)\right]^T\left[\hat{g}(x)-\hat{g}(y)-\mathcal{H}(x-y)\right]\le 0,\\ &\forall x,\ y\in\mathbb{R}^n.\end{aligned}\tag{13}$$

where $\mathcal{G}$ and $\mathcal{H}$ are constant matrices with appropriate dimensions.

Lemma 1 [37] *For a symmetric positive definite matrix $N\in\mathbb{R}^{n\times n}$, the following inequality holds for all differentiable function x in $[a,b]\to\mathbb{R}^n$:*

$$\begin{aligned}&\int_a^b\dot{x}^T(s)N\dot{x}(s)ds\\ &\quad\ge\frac{1}{b-a}\Omega_w^T diag(N,3N,5N)\Omega_w,\quad w=1,2,3.\end{aligned}\tag{14}$$

where

$$\begin{aligned}\Omega_1 &= x(b)-x(a),\\ \Omega_2 &= x(b)+x(a)-\frac{2}{b-a}\int_a^b x(s)ds,\\ \Omega_3 &= x(b)-x(a)+6\int_a^b\frac{x(s)}{b-a}ds-12\int_a^b\int_\theta^b\frac{x(s)}{(b-a)^2}dsd\theta.\end{aligned}$$

Lemma 2 [38] *Let $\mathfrak{M}>0$ be any constant matrix and for given scalars a and b with $a<b$, the following relation is well defined for any differentiable function φ in $[0,1]\to\mathbb{R}^n$:*

$$\begin{aligned}&\frac{b^2-a^2}{2}\int_{-a}^{-b}\int_{t+\theta}^{t}\dot{\varphi}^T(s)\mathfrak{M}\dot{\varphi}(s)dsd\theta\\ &\quad\le-\Omega_4^T\mathfrak{M}\Omega_4-2\Omega_5^T\mathfrak{M}\Omega_5,\end{aligned}\tag{15}$$

where

$$\begin{aligned}\Omega_4 &= (b-a)\varphi(t)-\int_{t-a}^{t-b}\varphi(s)ds,\\ \Omega_5 &= -\frac{(b-a)}{2}\varphi(t)-\int_{t-a}^{t-b}\varphi(s)ds\\ &\quad+\frac{3}{b-a}\int_{-a}^{-b}\int_{t+\theta}^{t}\varphi(s)dsd\theta.\end{aligned}$$

Lemma 3 [39] *For a given matrix $G>0$, given scalars a and b satisfying $a<b$, the following continuous differentiable inequalities hold for all x in $[a,b]\to\mathbb{R}^n$:*

$$\begin{aligned}(b-a)\int_a^b x^T(s)Gx(s)ds\ge&\left(\int_a^b x(s)ds\right)^T G\left(\int_a^b x(s)ds\right)\\ &+3\Omega_6^T G\Omega_6,\end{aligned}\tag{16}$$

where

$$\Omega_6=\int_a^b x(s)ds-\frac{2}{b-a}\int_a^b\int_a^s x(u)duds.$$

3 Main Results

A sufficient condition ensuring the stochastic mean-square stable for the error system (11) is provided. After that, a fault-tolerant control design methodology for T-S fuzzy MJCDNs is introduced.

Here are some notations provided for simplicity.

$$\Xi_1(t) = \Big[e^T(t) \quad e^T(t-\alpha(t)) \quad \frac{1}{\alpha(t)}\int_{t-\alpha(t)}^{t} e^T(s)\mathrm{d}s \quad \frac{1}{\alpha^2(t)}\int_{t-\alpha(t)}^{t}\int_{\theta}^{t} e^T(s)\mathrm{d}s\mathrm{d}\theta\Big],$$

$$\Xi_2(t) = \Big[e^T(t-\alpha(t)) \quad e^T(t-\alpha) \quad \frac{1}{\alpha-\alpha(t)}\int_{t-\alpha}^{t-\alpha(t)} \times e^T(s)\mathrm{d}s \quad \frac{1}{(\alpha-\alpha(t))^2}\int_{t-\alpha}^{t}\int_{\theta}^{t} e^T(s)\mathrm{d}s\mathrm{d}\theta\Big],$$

$$\Xi_3(t) = \Big[e^T(t) \quad \frac{1}{\alpha}\int_{t-\alpha}^{t} e^T(s)\mathrm{d}s \quad \frac{1}{\alpha^2}\int_{-\alpha}^{0}\int_{t+\theta}^{t} e^T(s)\mathrm{d}s\mathrm{d}\theta\Big],$$

$$\Xi_4(t) = \Big[\frac{1}{\alpha(t)}\int_{t-\alpha(t)}^{t} e^T(s)\mathrm{d}s \quad \frac{1}{\alpha^2(t)}\int_{t-\alpha(t)}^{t}\int_{\theta}^{t} e^T(s)\mathrm{d}s\mathrm{d}\theta\Big],$$

$$\Xi_5(t) = \Big[\frac{1}{\alpha-\alpha(t)}\int_{t-\alpha}^{t-\alpha(t)} e^T(s)\mathrm{d}s \quad \frac{1}{(\alpha-\alpha(t))^2}\int_{t-\alpha}^{t}\int_{\theta}^{t} e^T(s)\mathrm{d}s\mathrm{d}\theta\Big].$$

$$\Psi(t) = \Big[e^T(t) \quad e^T(t-\alpha(t)) \quad e^T(t-\alpha) \quad \hat{g}^T(e(t)) \quad \dot{e}^T(t) \quad \frac{1}{\alpha(t)}\int_{t-\alpha(t)}^{t} e^T(s)\mathrm{d}s \quad \frac{1}{\alpha-\alpha(t)}\int_{t-\alpha}^{t-\alpha(t)} e^T(s)\mathrm{d}s \quad \frac{1}{\alpha}\int_{t-\alpha}^{t} e^T(s)\mathrm{d}s \quad \frac{1}{\alpha^2(t)}\int_{t-\alpha(t)}^{t}\int_{\theta}^{t} e^T(s)\mathrm{d}s\mathrm{d}\theta \quad \frac{1}{(\alpha-\alpha(t))^2}\int_{t-\alpha}^{t}\int_{\theta}^{t} e^T(s)\mathrm{d}s\mathrm{d}\theta \quad \frac{1}{\alpha^2}\int_{-\alpha}^{0}\int_{t+\theta}^{t} e^T(s)\mathrm{d}s\mathrm{d}\theta\Big].$$

Theorem 1 *Let $\alpha, \lambda, \kappa, \varepsilon > 0$ are given scalars. The error system MJCDNs (11) is stochastic mean-square stable, if there exist positive definite matrices P_p (for each $p, q \in \mathcal{F}$), Q, T, U, Z, X for any matrix M with appropriate dimensions, and positive diagonal matrices $\bar{F}$ and $\bar{S}$ such that the following LMIs hold;*

$$\aleph_{\ell,p} = \begin{bmatrix} \xi^{11} & \xi^{12} & \xi^{13} \\ * & \xi^{22} & \xi^{23} \\ * & * & \xi^{33} \end{bmatrix} < 0, \tag{17}$$

where,

$$\xi^{11} = \begin{bmatrix} \eta_1 & \eta_2 & \eta_3 \\ \eta_4 & \eta_5 & \eta_6 \\ \eta_7 & \eta_8 & \eta_9 \end{bmatrix},$$

$$\xi^{12} = \begin{bmatrix} (I_N \otimes M)(I_N \otimes C_{\ell p}) + \varepsilon\bar{S} & \eta_{10} & -24(I_N \otimes Z) \\ 0 & 0 & 36(I_N \otimes Z) \\ 0 & 0 & 0 \end{bmatrix},$$

$$\xi^{13} = \begin{bmatrix} 0 & 0 & 60(I_N \otimes Z) & 0 & 3\alpha(I_N \otimes X) \\ -24(I_N \otimes Z) & 0 & -60(I_N \otimes Z) & 60(I_N \otimes Z) & 0 \\ 36(I_N \otimes Z) & 0 & 0 & -60(I_N \otimes Z) & 0 \end{bmatrix},$$

$$\xi^{22} = \begin{bmatrix} -\varepsilon\bar{I} & 0 & 0 \\ (I_N \otimes M)(I_N \otimes C_{\ell p}) & \eta_{11} & 0 \\ 0 & 0 & -192(I_N \otimes Z) + 4(I_N \otimes U) \end{bmatrix},$$

$$\xi^{23} = \begin{bmatrix} 0\,0 & 0 & 0\,0 \\ 0\,0 & 0 & 0\,0 \\ 0\,0\;360(I_N \otimes Z) - 6(I_N \otimes U) & & 0\,0 \end{bmatrix},$$

$$\xi^{33} = \begin{bmatrix} -192(I_N \otimes Z) + 4(I_N \otimes U) & 0 & 0 & 360(I_N \otimes Z) - 6(I_N \otimes U) & 0 \\ 0 & -3(I_N \otimes X) & 0 & 0 & 6(I_N \otimes X) \\ 0 & 0 & \eta_{12} & 0 & 0 \\ 360(I_N \otimes Z) - 6(I_N \otimes U) & 0 & 0 & -720(I_N \otimes Z) + 12(I_N \otimes U) & 0 \\ 0 & 6(I_N \otimes X) & 0 & 0 & -18(I_N \otimes X) \end{bmatrix}$$

with

$$\eta_1 = (I_N \otimes Q) + (I_N \otimes T) + \alpha(I_N \otimes U) + \sum_{q=1}^{\mathcal{N}}(I_N \otimes \pi_{pq})(I_N \otimes P_q) - 9(I_N \otimes Z) - \frac{3\alpha^2}{2}(I_N \otimes X) - \varepsilon\bar{F} - \varepsilon\bar{S} + 2(I_N \otimes M)(I_N \otimes R_{\ell p}) + 2(I_N \otimes M)(I_N \otimes W_{\ell p})\mathfrak{F}_{0p}(I + L_p)K_{vp},$$

$$\eta_2 = 3(I_N \otimes Z) + \kappa(I_N \otimes M)(\tilde{\Lambda}_{\ell p} \otimes \tilde{D}_{\ell p}),$$

$$\eta_3 = 0,$$

$$\eta_5 = -(1-\lambda)(I_N \otimes Q) - 18(I_N \otimes Z),$$

$$\eta_6 = 3(I_N \otimes Z), \quad \eta_9 = -(I_N \otimes T) - 9(I_N \otimes Z),$$

$$\eta_{10} = 2(I_N \otimes P_p) - (I_N \otimes M) + (I_N \otimes M)(I_N \otimes R_{\ell p}) + (I_N \otimes M)(I_N \otimes W_{\ell p})\mathfrak{F}_{0p}(I + L_p)K_{vp},$$

$$\eta_{11} = \alpha^2(I_N \otimes Z) + \frac{\alpha^2}{2}(I_N \otimes X) - 2(I_N \otimes M),$$

$$\eta_{12} = -720(I_N \otimes Z) + 12(I_N \otimes U).$$

Proof The chosen Lyapunov-Krasovskii functional for the system (11) would be:

$$V(e_t) = V_1(e_t) + V_2(e_t) + V_3(e_t) + V_4(e_t), \tag{18}$$

where

$$V_1(e_t) = e^T(t)(I_N \otimes P_p)e(t),$$

$$V_2(e_t) = \int_{t-\alpha(t)}^{t} e^T(s)(I_N \otimes Q)e(s)\mathrm{d}s + \int_{t-\alpha}^{t} e^T(s)(I_N \otimes T)e(s)\mathrm{d}s,$$

$$V_3(e_t) = \alpha\int_{-\alpha}^{0}\int_{t+\theta}^{t} \dot{e}^T(s)(I_N \otimes Z)\dot{e}(s)\mathrm{d}s\mathrm{d}\theta + \int_{-\alpha}^{0}\int_{t+\theta}^{t} e^T(s)(I_N \otimes U)e(s)\mathrm{d}s\mathrm{d}\theta,$$

$$V_4(e_t) = \int_{-\alpha}^{0}\int_{\nu}^{0}\int_{t+\theta}^{t} \dot{e}^T(s)(I_N \otimes X)\dot{e}(s)\mathrm{d}s\mathrm{d}\theta\mathrm{d}\nu.$$

Define $\mathfrak{L}$ be the weak infinitesimal operator associated with the random process $(e_t, \tau(t)), t \geq 0$,

$$\mathfrak{L}V_1(e_t) = 2e^T(t)(I_N \otimes P_p)\dot{e}(t) + \sum_{q=1}^{\mathcal{N}}(I_N \otimes \pi_{pq})e^T(t)(I_N \otimes P_q)e(t),$$

$$= 2e^T(t)(I_N \otimes P_p) \sum_{\ell=1}^{m}\psi_\ell(\omega(t))\sum_{v=1}^{m}\psi_\ell(\omega(t))\{(I_N \otimes R_{\ell p})e(t) + (I_N \otimes C_{\ell p})\hat{g}(e(t)) + \kappa(\tilde{\Lambda}_{\ell p} \otimes \tilde{D}_{\ell p})e(t-\alpha(t)) + (I_N \otimes W_{\ell p})\mathfrak{F}_{0p}(I + L_p)K_{vp}e(t)\} + \sum_{q=1}^{\mathcal{N}}(I_N \otimes \pi_{pq})e^T(t)(I_N \otimes P_q)e(t), \tag{19}$$

$$\mathfrak{L}V_2(e_t) \leq e^T(t)((I_N \otimes Q) + (I_N \otimes T))e(t) - e^T(t-\alpha)(I_N \otimes T)e(t-\alpha) - (1-\lambda)e^T(t-\alpha(t))(I_N \otimes Q)e(t-\alpha(t)), \tag{20}$$

$$\mathfrak{L}V_3(e_t) = \alpha^2\dot{e}^T(t)(I_N \otimes Z)\dot{e}(t) - \alpha\int_{t-\alpha}^{t}\dot{e}^T(s)(I_N \otimes Z)\dot{e}(s)\mathrm{d}s + \alpha e^T(t)(I_N \otimes U)e(t) - \int_{t-\alpha}^{t} e^T(s)(I_N \otimes U)e(s)\mathrm{d}s, \tag{21}$$

$$\mathfrak{L}\dot{V}_4(e_t) = \frac{\alpha^2}{2}\dot{e}^T(t)(I_N \otimes X)\dot{e}(t) - \int_{-\alpha}^{0}\int_{t+\nu}^{t}\dot{e}^T(s)(I_N \otimes X)\dot{e}(s)\mathrm{d}s\mathrm{d}\nu. \tag{22}$$

The integral terms from (21) can be reformulated as

$$-\alpha\int_{t-\alpha}^{t}\dot{e}^T(s)(I_N \otimes Z)\dot{e}(s)\mathrm{d}s = -\Big[\alpha(t)\int_{t-\alpha(t)}^{t}\dot{e}^T(s)(I_N \otimes Z)\dot{e}(s)\mathrm{d}s + (\alpha - \alpha(t))\int_{t-\alpha}^{t-\alpha(t)}\dot{e}^T(s)(I_N \otimes Z)\dot{e}(s)\mathrm{d}s\Big].$$

By using Lemma 1, from the above, we can get

$$-\alpha(t)\int_{t-\alpha(t)}^{t}\dot{e}^T(s)(I_N \otimes Z)\dot{e}(s)\mathrm{d}s \leq \Xi_1^T(t)\mathcal{Z}_1\Xi_1(t), \tag{23}$$

where

$$\mathcal{Z}_1 = \begin{bmatrix} -9(I_N \otimes Z) & 3(I_N \otimes Z) & -24(I_N \otimes Z) & 60(I_N \otimes Z) \\ * & -9(I_N \otimes Z) & 36(I_N \otimes Z) & -60(I_N \otimes Z) \\ * & * & -192(I_N \otimes Z) & 360(I_N \otimes Z) \\ * & * & * & -720(I_N \otimes Z) \end{bmatrix}$$

and

$$-(\alpha - \alpha(t))\int_{t-\alpha}^{t-\alpha(t)}\dot{e}^T(s)(I_N \otimes Z)\dot{e}(s)\mathrm{d}s \leq \Xi_2^T(t)\mathcal{Z}_2\Xi_2(t), \tag{24}$$

where

$$\mathcal{Z}_2 = \begin{bmatrix} -9(I_N \otimes Z) & 3(I_N \otimes Z) & -24(I_N \otimes Z) & 60(I_N \otimes Z) \\ * & -9(I_N \otimes Z) & 36(I_N \otimes Z) & -60(I_N \otimes Z) \\ * & * & -192(I_N \otimes Z) & 360(I_N \otimes Z) \\ * & * & * & -720(I_N \otimes Z) \end{bmatrix}$$

$$-\alpha \int_{t-\alpha}^{t} \dot{e}^T(s)(I_N \otimes Z)\dot{e}(s)\mathrm{d}s \le \Xi_1^T(t)\mathcal{Z}_1\Xi_1(t) + \Xi_2^T(t)\mathcal{Z}_2\Xi_2(t). \quad (25)$$

By using Lemma 2, the integral terms in (22) are rewritten as

$$\begin{aligned} &\int_{-\alpha}^{0}\int_{t+\nu}^{t} \dot{e}^T(s)(I_N \otimes X)\dot{e}(s)\mathrm{d}s \\ &\le -\Omega_4^T\mathcal{X}\Omega_4 - 2\Omega_5^T\mathcal{X}\Omega_5 \\ &\le \Xi_3^T(t)\mathcal{X}\Xi_3(t), \end{aligned} \quad (26)$$

where Ω_4 and Ω_5 defined from Lemma 2

$$\mathcal{X} = \begin{bmatrix} -\frac{3\alpha^2}{2}(I_N \otimes X) & 0 & 3\alpha(I_N \otimes X) \\ * & -3(I_N \otimes X) & 6(I_N \otimes X) \\ * & * & -18(I_N \otimes X) \end{bmatrix},$$

By using Lemma 3, the integral terms in (21) are written as

$$\begin{aligned} &\int_{t-\alpha}^{t} e^T(s)(I_N \otimes U)e(s)\mathrm{d}s\mathrm{d}\theta \\ &= \int_{t-\alpha(t)}^{t} e^T(s)(I_N \otimes U)e(s)\mathrm{d}s\mathrm{d}\theta \\ &\quad + \int_{t-\alpha}^{t-\alpha(t)} e^T(s)(I_N \otimes U)e(s)\mathrm{d}s\mathrm{d}\theta, \end{aligned}$$

From the above we can get,

$$\int_{t-\alpha(t)}^{t} e^T(s)(I_N \otimes U)e(s)\mathrm{d}s\mathrm{d}\theta \le \Xi_4^T(t)\mathcal{U}_1\Xi_4(t), \quad (27)$$

where

$$\mathcal{U}_1 = \begin{bmatrix} 4(I_N \otimes U) & -6(I_N \otimes U) \\ * & 12(I_N \otimes U) \end{bmatrix},$$

$$\int_{t-\alpha}^{t-\alpha(t)} e^T(s)(I_N \otimes U)e(s)\mathrm{d}s\mathrm{d}\theta \le \Xi_5^T(t)\mathcal{U}_2\Xi_5(t), \quad (28)$$

where

$$\mathcal{U}_2 = \begin{bmatrix} 4(I_N \otimes U) & -6(I_N \otimes U) \\ * & 12(I_N \otimes U) \end{bmatrix},$$

Moreover, the inequality that follows can be taken for any $\varepsilon > 0$,

$$b(t) = \varepsilon \begin{bmatrix} e(t) \\ \hat{g}(e(t)) \end{bmatrix}^T \begin{bmatrix} \bar{F} & \bar{S} \\ * & I \end{bmatrix} \begin{bmatrix} e(t) \\ \hat{g}(e(t)) \end{bmatrix} \le 0, \quad (29)$$

where

$$\bar{F} = \frac{(I_N \otimes \mathcal{G})^T(I_N \otimes \mathcal{H})}{2} + \frac{(I_N \otimes \mathcal{H})^T(I_N \otimes \mathcal{G})}{2},$$
$$\bar{S} = -\frac{(I_N \otimes \mathcal{G})^T + (I_N \otimes \mathcal{H})^T}{2},$$

where $\mathcal{G}$ and $\mathcal{H}$ are constant matrices with appropriate dimensions.

Then, for any appropriate dimension matrices M, it is evident that the equation holds:

$$\begin{aligned} 0 = 2\Big[e^T(t) + \dot{e}^T(t)\Big](I_N \otimes M)\Big[&-\dot{e}(t) \\ &+ \sum_{\ell=1}^{m}\psi_\ell(\omega(t))\sum_{v=1}^{m}\psi_v(\omega(t))\{(I_N \otimes R_{\ell p})e(t) \\ &+ (I_N \otimes C_{\ell p})\hat{g}(e(t)) + \kappa(\tilde{\Lambda}_{\ell p} \otimes \tilde{D}_{\ell p})e(t-\alpha(t)) \\ &+ (I_N \otimes W_{\ell p})\mathfrak{F}_{0p}(I + L_p)K_{vp}e(t)\}\Big]. \end{aligned} \quad (30)$$

Combining from (19) to (30), we get

$$\begin{aligned} \mathfrak{L}V(e_t) \le\ & 2e^T(t)(I_N \otimes P_p)\dot{e}(t) \\ &+ \sum_{q=1}^{\mathcal{N}}(I_N \otimes \pi_{pq})e^T(t)(I_N \otimes P_q)e(t) \\ &+ e^T((I_N \otimes Q) + (I_N \otimes T))e(t) \\ &- (1-\lambda)e^T(t-\alpha(t))(I_N \otimes Q)e(t-\alpha(t)) \\ &- e^T(t-\alpha)(I_N \otimes T)e(t-\alpha) \\ &+ \alpha\dot{e}^T(t)(I_N \otimes Z)\dot{e}(t) + \Xi_1^T(t)\mathcal{Z}_1\Xi_1(t) \\ &+ \Xi_2^T(t)\mathcal{Z}_2\Xi_2(t) + \frac{\alpha^2}{2}\dot{e}^T(t)(I_N \otimes X)\dot{e}(t) \\ &+ \Xi_3^T(t)\mathcal{X}\Xi_3(t) + \alpha e^T(t)(I_N \otimes U)e(t) \\ &+ \Xi_4^T(t)\mathcal{U}_1\Xi_4(t) + \Xi_5^T(t)\mathcal{U}_2\Xi_5(t) \\ &- \varepsilon e^T(t)\bar{F}e(t) - \varepsilon\hat{g}(e(t))\bar{S}e(t) \\ &- \varepsilon e^T(t)\bar{S}\hat{g}(e(t)) - \varepsilon\hat{g}^T(e(t))I\hat{g}(e(t)) \\ &- 2e^T(t)(I_N \otimes M)\dot{e}(t) \\ &+ 2e^T(t)(I_N \otimes M)(I_N \otimes R_{\ell p})e(t) \\ &+ 2e^T(t)(I_N \otimes M)(I_N \otimes C_{\ell p})\hat{g}(e(t)) \\ &+ 2e^T(t)\kappa(I_N \otimes M)(\tilde{\Lambda}_{\ell p} \otimes \tilde{D}_{\ell p})e(t-\alpha(t)) \\ &+ 2e^T(t)(I_N \otimes M)(I_N \otimes W_{\ell p})\mathfrak{F}_{0p}(I+L_p)K_{vp}e(t) \\ &- 2\dot{e}^T(t)(I_N \otimes M)\dot{e}(t) \end{aligned}$$

$$
\begin{aligned}
&+2\dot{e}^T(t)(I_N\otimes M)(I_N\otimes R_{\ell p})e(t)\\
&+2\dot{e}^T(t)(I_N\otimes M)(I_N\otimes C_{\ell p})\hat{g}(e(t))\\
&+2\kappa\dot{e}^T(t)(I_N\otimes M)(\tilde{\Lambda}_{\ell p}\otimes\tilde{D}_{\ell p})e(t-\alpha(t))\\
&+2\dot{e}^T(t)(I_N\otimes M)(I_N\otimes W_{\ell p})\mathfrak{F}_{0p}(I+L_p)K_{vp}e(t),
\end{aligned}
\tag{31}
$$

It follows from (30) and (31), we get

$$
\mathfrak{L}V(e_t)\le\Psi^T(t)\begin{bmatrix}\xi_p^{11} & \xi_p^{12} & \xi_p^{13}\\ * & \xi_p^{22} & \xi_p^{23}\\ * & * & \xi_p^{33}\end{bmatrix}\Psi(t). \tag{32}
$$

and a scalar $\varsigma>0$ exists to affirm that for each $p\in\mathcal{F}$

$$
\mathfrak{L}V(e_t)\le-\varsigma|(e_t)|^2, \tag{33}
$$

it can be proved that

$$
\varrho\left\{\int_0^\infty e^T(t,e(0),\tau(0))e(t,e(0),\tau(0))\mathrm{d}t|e(0),\tau(0)\right\}<\infty. \tag{34}
$$

By the Definition 1, the error system (11) is stochastic mean-square stable, which implies the master and slave system (3) and (4) are synchronized. This concludes the proof. □

Theorem 2 *For given scalars α, λ, κ, and $\varepsilon>0$. The error system for MJCDNs (11) is considered to be stochastic mean-square stable if there exist positive definite matrices $\bar{P}_p$ for all $p,q\in\mathcal{F}$, along with $\bar{Q}$, $\bar{T}$, $\bar{U}$, $\bar{Z}$, and $\bar{X}$ for any matrices $\mathcal{M}$ and Y_p with appropriate dimensions. Additionally, positive diagonal matrices $\widehat{F}$ and $\widehat{S}$ must satisfy the following LMIs:*

$$
\bar{\aleph}_{\ell,p}=\begin{bmatrix}\bar{\xi}^{11} & \bar{\xi}^{12} & \bar{\xi}^{13}\\ * & \bar{\xi}^{22} & \bar{\xi}^{23}\\ * & * & \bar{\xi}^{33}\end{bmatrix}<0, \tag{35}
$$

where

$$
\bar{\xi}^{11}=\begin{bmatrix}\bar{\eta}_1 & \bar{\eta}_2 & \bar{\eta}_3\\ \bar{\eta}_4 & \bar{\eta}_5 & \bar{\eta}_6\\ \bar{\eta}_7 & \bar{\eta}_8 & \bar{\eta}_9\end{bmatrix},
$$

$$
\bar{\xi}^{12}=\begin{bmatrix}\mathcal{M}(I_N\otimes C_{\ell p})+\varepsilon\widehat{S} & \bar{\eta}_{10} & -24(I_N\otimes\bar{Z})\\ 0 & 0 & 36(I_N\otimes\bar{Z})\\ 0 & 0 & 0\end{bmatrix},
$$

$$
\bar{\xi}^{13}=\begin{bmatrix}0 & 0 & 60(I_N\otimes\bar{Z}) & 0 & 3\alpha(I_N\otimes\bar{X})\\ -24(I_N\otimes\bar{Z}) & 0 & 60(I_N\otimes\bar{Z}) & 60(I_N\otimes\bar{Z}) & 0\\ 36(I_N\otimes\bar{Z}) & 0 & 0 & 60(I_N\otimes\bar{Z}) & 0\end{bmatrix},
$$

$$
\bar{\xi}^{22}=\begin{bmatrix}-\varepsilon I & 0 & 0\\ \mathcal{M}(I_N\otimes C_{\ell p}) & \bar{\eta}_{11} & 0\\ 0 & 0 & -192(I_N\otimes\bar{Z})+4(I_N\otimes\bar{U})\end{bmatrix},
$$

$$
\xi^{23}=\begin{bmatrix}0\,0 & 0 & 0\,0\\ 0\,0 & 0 & 0\,0\\ 0\,0\ 360(I_N\otimes\bar{Z})-6(I_N\otimes\bar{U}) & 0\,0\end{bmatrix},
$$

$$
\bar{\xi}^{33}=\begin{bmatrix}-192(I_N\otimes\bar{Z})+4(I_N\otimes\bar{U}) & 0 & 0 & 360(I_N\otimes\bar{Z})-6(I_N\otimes\bar{U}) & 0\\ 0 & -3(I_N\otimes\bar{X}) & 0 & 0 & 6(I_N\otimes\bar{X})\\ 0 & 0 & \bar{\eta}_{12} & 0 & 0\\ 360(I_N\otimes\bar{Z})-6(I_N\otimes\bar{U}) & 0 & 0 & -720(I_N\otimes\bar{Z})+12(I_N\otimes\bar{U}) & 0\\ 0 & 6(I_N\otimes\bar{X}) & 0 & 0 & -18(I_N\otimes\bar{X})\end{bmatrix}
$$

with

$$\begin{aligned}
\bar{\eta}_1 &= (I_N \otimes \bar{Q}) + (I_N \otimes \bar{T}) + \alpha(I_N \otimes \bar{U}) \\
&\quad + \sum_{q=1}^{\mathcal{N}} (I_N \otimes \pi_{pq})(I_N \otimes \bar{P}_q) \\
&\quad - 9(I_N \otimes \bar{Z}) - \frac{3\alpha^2}{2}(I_N \otimes \bar{X}) \\
&\quad - \varepsilon\widehat{F} - \varepsilon\widehat{S} + 2\mathcal{M}(I_N \otimes R_{\ell p}) \\
&\quad + 2(I_N \otimes W_{\ell p})\mathfrak{F}_{0p}(I + L_p)Y_p, \\
\bar{\eta}_2 &= 3(I_N \otimes \bar{Z}) + \mathcal{M}\kappa(\tilde{\Lambda}_{\ell p} \otimes \tilde{D}_{\ell p}), \\
\bar{\eta}_5 &= -(1-\lambda)(I_N \otimes \bar{Q}) - 18(I_N \otimes \bar{Z}), \\
\bar{\eta}_6 &= 3(I_N \otimes \bar{Z}), \\
\bar{\eta}_9 &= -(I_N \otimes \bar{T}) - 9(I_N \otimes \bar{Z}), \\
\bar{\eta}_{10} &= \mathcal{M}(I_N \otimes R_{\ell p}) \\
&\quad + (I_N \otimes W_{\ell p})\mathfrak{F}_{0p}(I + L_p)Y_p + 2(I_N \otimes \bar{P}_p) - \mathcal{M}, \\
\bar{\eta}_{11} &= \alpha^2(I_N \otimes \bar{Z}) + \frac{\alpha^2}{2}(I_N \otimes \bar{X}) \\
&\quad - 2\mathcal{M}, \qquad \bar{\eta}_{12} = -720(I_N \otimes \bar{Z}) + 12(I_N \otimes \bar{U}).
\end{aligned}$$

Then, the fault-tolerant control is designed as $K_{vp} = Y_{vp}\mathcal{M}^{-1}$.

Proof The matrix variables required are defined $\mathcal{M} = M^{-1}$, $\bar{P}_p = \mathcal{M}P_p\mathcal{M}$, $\bar{Q} = \mathcal{M}Q\mathcal{M}$, $\bar{T} = \mathcal{M}T\mathcal{M}$, $\bar{U} = \mathcal{M}U\mathcal{M}$, $\bar{Z} = \mathcal{M}Z\mathcal{M}$, $\bar{X} = \mathcal{M}X\mathcal{M}$, $\widehat{F} = \mathcal{M}\bar{F}\mathcal{M}$, $\widehat{S} = \mathcal{M}\bar{S}\mathcal{M}$, and $Y_{vp} = K_{vp}\mathcal{M}^T$. By performing pre- and post-multiply by $diag\,[\mathcal{M}\ \ \mathcal{M}\ \ \mathcal{M}\ \ \mathcal{M}\ \ \mathcal{M}\ \ \mathcal{M}\ \ \mathcal{M}\ \ \mathcal{M}\ \ \mathcal{M}\ \ \mathcal{M}\ \ \mathcal{M}]$ in (17), the resulting LMI (35) is obtained. This concludes the proof. □

Remark 2 If the system (11) does not include fuzzy components, it can be written as the following equation:

$$\begin{aligned}
\dot{e}(t) =& (I_N \otimes R_p)e(t) + (I_N \otimes C_p)\hat{g}(e(t)) \\
&+ \kappa(\tilde{\Lambda}_p \otimes \tilde{D}_p)e(t - \alpha(t)) \\
&+ (I_N \otimes W_p)\mathfrak{F}_{0p}(I + L_p)K_p e(t), \qquad (36)
\end{aligned}$$

then it is clear from the proof of Theorem 2 that the system holds.

Remark 3 Primarily, computational complexity will be a big issue based on how large are the LMIs. However, large size of LMIs yields better performance. The results in Theorems are derived based on the construction of proper LKF with double and triple, integral terms in $V_3(e_t)$, $V_4(e_t)$, and by using new integral inequality techniques which produce tighter bounds than what the existing ones such as the Reciprocally convex approach. As a result, some computational complexity can occur in the proposed criterion. It should be mentioned that the obtained maximum allowable bounds α are less conservative than the existing ones in the literature, it is easy to see in Table 2. To minimize computation complexity burden and time computation, we will be using Finsler's Lemma in our future work to reduce the number of decision variables. The above comments have been included in the revised manuscript.

Remark 4 Generally, synchronization scheme with fault-tolerant control (FTC), T-S fuzzy, and Markovian jumping problems are not simply applied to complex dynamical networks (CDNs). Some research publications have tackled such problems. It is noted that the authors of [23] investigated the fault-tolerant control problem for Markov jump nonlinear systems in the presence of actuator faults. Moreover, the work presented in [27] explored the FTC synchronization control for CDN with semi-markov jump topology. Further, in [3], the authors explored the pinning synchronization for delayed CDNs with Markovian jump modes. Also, the research in [28] focused on the analysis of synchronization of T-S fuzzy Markovian jump CDNs. The model considered in the present study is more practical than that proposed by [3,23,27,28], because they consider usual relevant control has been studied with CDNs based on stabilization conditions, but in this paper, we consider a FTC, with the combination of synchronization approach, coupling delay, T-S fuzzy rules, and Markovian jumping modes. Due to the many real-life applications, the combined study of CDNs and fuzzy FTC to the system model is more important. The purpose of this study is to establish synchronization of these complex networks achieved through FTC by applying the Lyapunov functional theory and to apply a practical application of the Chua circuit with time delay. Furthermore, fault-tolerant control design is gaining more importance as it can maintain system stability and preserve the performance of considered systems in the presence of actuator faults. Hence, the comprehensive analysis of the proposed control strategy in the presence of multiple challenges demonstrates the system's relevance and applicability to real-world scenarios.

4 Numerical Examples

This section includes numerical examples illustrating the effectiveness of the proposed strategy in achieving synchronization for MJCDNs (3) and (4) with coupling delay and T-S fuzzy using fault-tolerant control.

Example 1 Consider a T-S fuzzy MJCDNs (3) and (4), which is described by the following parameters: $N = 5$ nodes, two

fuzzy rules and 2 jumping mode ($p = 1, 2$):

$$R_{11} = \begin{bmatrix} -4 & 2 & 0 \\ 1 & -2 & 0 \\ 0.2 & 1 & -6 \end{bmatrix}, \quad R_{12} = \begin{bmatrix} -3 & 2 & 0.3 \\ 0 & -2 & 0 \\ 0.2 & 1 & -5 \end{bmatrix},$$

$$C_{11} = \begin{bmatrix} 1 & 0.2 & 0 \\ 0 & 0.3 & 0 \\ 0 & 1 & 0.1 \end{bmatrix}, \quad C_{12} = \begin{bmatrix} 1.2 & 3 & 0.2 \\ 0 & -2.1 & 0 \\ 0 & 1 & -0.1 \end{bmatrix},$$

$$W_{11} = \begin{bmatrix} 0.1 & 0.3 & 0.4 \\ 0.5 & -2 & 0 \\ 0 & 1 & 0.8 \end{bmatrix}, \quad W_{12} = \begin{bmatrix} 1.3 & 0.4 & 0 \\ 0 & 0.62 & 0 \\ 0 & 1 & 0.4 \end{bmatrix},$$

$$\tilde{\Lambda}_{11} = \begin{bmatrix} 0.1 & 0.4 & 0 \\ 0 & 0.12 & 0 \\ 0 & 1 & 0.6 \end{bmatrix}, \quad \tilde{\Lambda}_{12} = \begin{bmatrix} 1.3 & 0.8 & 0 \\ 0 & 0.6 & 0 \\ 0 & 1 & 0.9 \end{bmatrix}.$$

$$\begin{aligned} \mathfrak{F}_{01} = diag\{&0.4, \quad 0.3, \quad 0.5, \quad 0.6, \quad 0.15, \\ &0.25, \quad 0.35, \quad 0.26, \quad 0.14, \quad 0.58, \\ &0.22, \quad 0.45, \quad 0.5, \quad 0.6, \quad 0.4\}, \end{aligned}$$

$$R_{21} = \begin{bmatrix} -1.5 & 1.05 & 2 \\ 0 & 5 & 0 \\ 1 & 0.1 & -2.3 \end{bmatrix}, \quad R_{22} = \begin{bmatrix} -5.2 & 0.6 & 0.2 \\ 0 & -2.2 & 0 \\ 0 & 0 & -6.3 \end{bmatrix},$$

$$C_{21} = \begin{bmatrix} -1.5 & 0.4 & 0 \\ 0.3 & -2.6 & 0 \\ 0 & 1 & -6.2 \end{bmatrix}, \quad C_{22} = \begin{bmatrix} 1.5 & 0 & 0.6 \\ 0.3 & -2.5 & 0 \\ 0 & 1 & 6 \end{bmatrix},$$

$$W_{21} = \begin{bmatrix} 1.2 & 1.3 & 0 \\ 0 & 3.1 & 0 \\ 0.6 & 0 & -1.5 \end{bmatrix}, \quad W_{22} = \begin{bmatrix} -1.2 & 0.5 & 0 \\ 0 & 5 & 0 \\ 0.2 & 0 & -1 \end{bmatrix},$$

$$\tilde{\Lambda}_{21} = \begin{bmatrix} 6 & 0 & 0 \\ 0.1 & -4 & 0.1 \\ 0 & 1 & -1 \end{bmatrix}, \quad \tilde{\Lambda}_{22} = \begin{bmatrix} 0.3 & 0.1 & 0 \\ 0 & 3 & 0 \\ 0.1 & 1 & 2 \end{bmatrix}.$$

$$\begin{aligned} \mathfrak{F}_{02} = diag\{&0.1, \quad 0.3, \quad 0.2, \quad 0.4, \quad 0.25, \\ &0.75, \quad 0.6, \quad 0.46, \quad 0.44, \\ &0.68, \quad 0.72, \quad 0.75, \quad 0.35, \quad 0.64, \quad 0.74\}, \end{aligned}$$

where $\hat{g}(e(t)) = \tanh(e(t))$, and the outer coupling matrices are

$$\tilde{D}_{11} = \begin{bmatrix} -0.5 & 0.4 & 0.3 & 0.2 & 0.4 \\ 0 & -0.1 & 0.1 & -1.2 & 0.1 \\ 0.6 & 0.4 & -0.4 & 0.2 & 0.4 \\ 0.4 & 0.5 & -0.2 & 0.1 & -0.1 \\ 0.5 & 0 & -0.5 & 0.4 & 0.8 \end{bmatrix},$$

$$\tilde{D}_{12} = \begin{bmatrix} -0.4 & 1.2 & 1.3 & -0.2 & -0.3 \\ 0.3 & 0.4 & 0.5 & -1.6 & 0.3 \\ 0.7 & 1.3 & -1.4 & 0.8 & 0.3 \\ 0.8 & 0.9 & -1.2 & -0.2 & -0.3 \\ 0.7 & -0.5 & -1.2 & 0.2 & -0.1 \end{bmatrix},$$

$$\tilde{D}_{21} = \begin{bmatrix} -1.2 & 0.1 & 2.1 & 0.4 & -0.7 \\ 0.4 & 1.3 & 0.3 & -1.5 & 0.6 \\ 1.4 & 1.2 & -1.6 & 0.1 & 0.5 \\ 0.7 & 0.3 & -1.7 & -1.7 & 0.4 \\ 0.3 & 0.6 & -1.4 & 0.6 & -0.8 \end{bmatrix},$$

$$\tilde{D}_{22} = \begin{bmatrix} -1.7 & 1.3 & 1.2 & -0.4 & -1.1 \\ 0.8 & 0.4 & 0.6 & -1.1 & 0.5 \\ 0.5 & 1.7 & -1.6 & 1.8 & 0.3 \\ 0.1 & 1.9 & -0.2 & -1.2 & -2.3 \\ 0.2 & -1.5 & -0.2 & 2.2 & -1.1 \end{bmatrix}.$$

The fuzzy membership functions are taken as $\psi_1(\omega(t)) = (\sin(\omega(t)) - \hat{\sigma}(\omega(t)))/\omega(t)(1-\hat{\sigma})$, $\psi_2(\omega(t)) = (\omega(t) - \sin(\omega(t)))/\omega(t)(1-\hat{\sigma})$, where $\hat{\sigma} > 0$, transition matrix $\pi = \begin{bmatrix} 0.3 & -0.3 \\ -0.5 & 0.5 \end{bmatrix}$, $\alpha = 1.6$, $\lambda = 0.8$, $\varepsilon = 0.5$, and $\kappa = 0.1$. According to Theorem 2 in the LMI (35) and with the help of the Matlab LMI Toolbox, the control gain matrices can be derived using the specified matrix variables in the following manner:

$$\begin{aligned} K_{11} &= diag\{K_{1a}, K_{2a}, K_{3a}, K_{4a}, K_{5a}\}, \\ K_{12} &= diag\{K_{6a}, K_{7a}, K_{8a}, K_{9a}, K_{10a}\}, \\ K_{21} &= diag\{K_{11a}, K_{12a}, K_{13a}, K_{14a}, K_{15a}\}, \\ K_{22} &= diag\{K_{16a}, K_{17a}, K_{18a}, K_{19a}, K_{20a}\}, \end{aligned}$$

where

$$K_{1a} = \begin{bmatrix} -0.2628 & -0.6935 & 0.3717 \\ -0.0995 & -0.4116 & 0.2108 \\ 0.0622 & 0.2562 & -0.2885 \end{bmatrix},$$

$$K_{2a} = \begin{bmatrix} -0.2119 & -0.8224 & 0.4280 \\ -0.2033 & -1.0253 & 0.5246 \\ 0.1080 & 0.5704 & -0.6135 \end{bmatrix},$$

$$K_{3a} = \begin{bmatrix} -0.2319 & -0.6121 & 0.4534 \\ -0.0943 & -0.4180 & 0.2753 \\ 0.1074 & 0.4773 & -0.7922 \end{bmatrix},$$

$$K_{4a} = \begin{bmatrix} -0.2440 & -0.8546 & 0.4271 \\ -0.1736 & -0.7943 & 0.3840 \\ 0.0878 & 0.4054 & -0.3780 \end{bmatrix},$$

$$K_{5a} = \begin{bmatrix} -0.2355 & -0.5514 & 0.4456 \\ -0.0572 & -0.2015 & 0.1494 \\ 0.0826 & 0.2777 & -0.3845 \end{bmatrix},$$

$$K_{6a} = \begin{bmatrix} -0.0228 & 0.0540 & -0.0764 \\ -0.0630 & -0.5915 & 0.3876 \\ 0.0464 & 0.4880 & -0.6946 \end{bmatrix},$$

$$K_{7a} = \begin{bmatrix} -0.0140 & 0.0237 & -0.0419 \\ -0.1286 & -0.9895 & 0.5450 \\ 0.0764 & 0.6503 & -0.9849 \end{bmatrix},$$

$$K_{8a} = \begin{bmatrix} -0.0281 & 0.0283 & -0.0785 \\ -0.0625 & -0.5125 & 0.3333 \\ 0.0567 & 0.5485 & -1.1756 \end{bmatrix},$$

$$K_{9a} = \begin{bmatrix} -0.0132 & 0.0363 & -0.0506 \\ -0.0912 & -0.7119 & 0.4141 \\ 0.0581 & 0.4951 & -0.6878 \end{bmatrix},$$

$$K_{10a} = \begin{bmatrix} -0.0185 & 0.0310 & -0.0719 \\ -0.0266 & -0.2384 & 0.2104 \\ 0.0364 & 0.3709 & -0.7573 \end{bmatrix},$$

$$K_{11a} = \begin{bmatrix} -1.1783 & -1.1895 & 0.0933 \\ -0.1082 & -0.7613 & 0.1161 \\ 0.1544 & 1.7800 & -6.6846 \end{bmatrix},$$

$$K_{12a} = \begin{bmatrix} -0.3299 & -0.4695 & 0.0404 \\ -0.1532 & -1.0075 & 0.1817 \\ 0.0392 & 0.4526 & -1.9024 \end{bmatrix},$$

$$K_{13a} = \begin{bmatrix} -0.2063 & -0.2712 & 0.0473 \\ -0.0543 & -0.3408 & 0.0153 \\ 0.0851 & 0.8026 & -3.5334 \end{bmatrix},$$

$$K_{14a} = \begin{bmatrix} -0.1787 & -0.2348 & 0.0191 \\ -0.0287 & -0.1662 & 0.0125 \\ 0.0473 & 0.4660 & -1.8355 \end{bmatrix},$$

$$K_{15a} = \begin{bmatrix} -0.3702 & -0.4023 & 0.0035 \\ -0.0321 & -0.1940 & 0.0217 \\ 0.0428 & 0.4879 & -2.0166 \end{bmatrix},$$

$$K_{16a} = \begin{bmatrix} -0.2965 & -0.2798 & 0.0525 \\ -0.2798 & -2.2891 & 0.5300 \\ 0.0525 & 0.5300 & -1.8924 \end{bmatrix},$$

$$K_{17a} = \begin{bmatrix} -0.2797 & -0.3062 & 0.0521 \\ -0.3062 & -2.2385 & 0.4971 \\ 0.0521 & 0.4971 & -1.8546 \end{bmatrix},$$

$$K_{18a} = \begin{bmatrix} -0.2820 & -0.2904 & 0.0478 \\ -0.2904 & -2.1430 & 0.4412 \\ 0.0478 & 0.4412 & -1.7967 \end{bmatrix},$$

$$K_{19a} = \begin{bmatrix} -0.2848 & -0.3138 & 0.0559 \\ -0.3138 & -2.2730 & 0.5033 \\ 0.0559 & 0.5033 & -1.8488 \end{bmatrix},$$

$$K_{20a} = \begin{bmatrix} -0.2847 & -0.2900 & 0.0523 \\ -0.2900 & -2.1419 & 0.4745 \\ 0.0523 & 0.4745 & -1.8268 \end{bmatrix}.$$

Figures 1, 2, 3, 4, 5, 6, 7, 8, 9, 10, and 11 represent the state trajectories of the system (11) using random initial conditions. These figures illustrate the perfect synchronization of the states of both identical and isolated nodes, which underlines the effectiveness of the developed control strategy. To evaluate the efficiency of the method, we show the synchro-

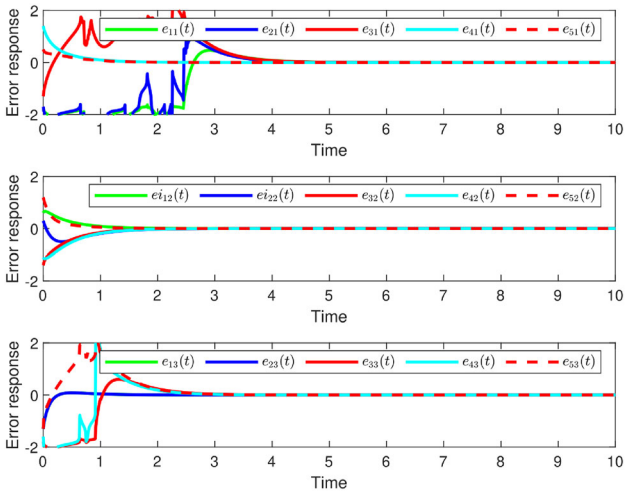

Fig. 1 State responses for the error system (11) for Example 1

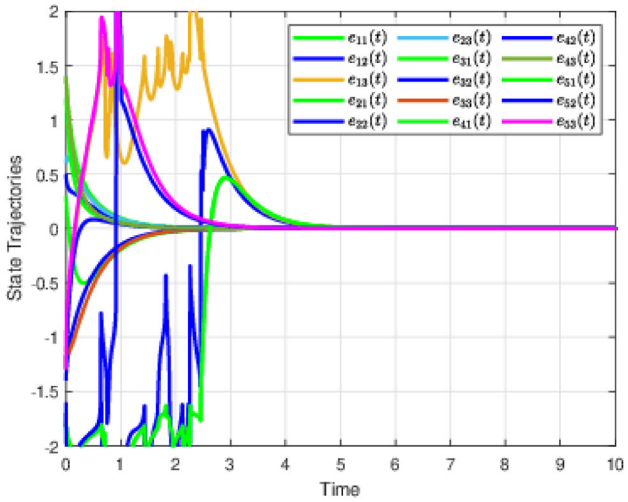

Fig. 2 State responses for the error system (11) for Example 1

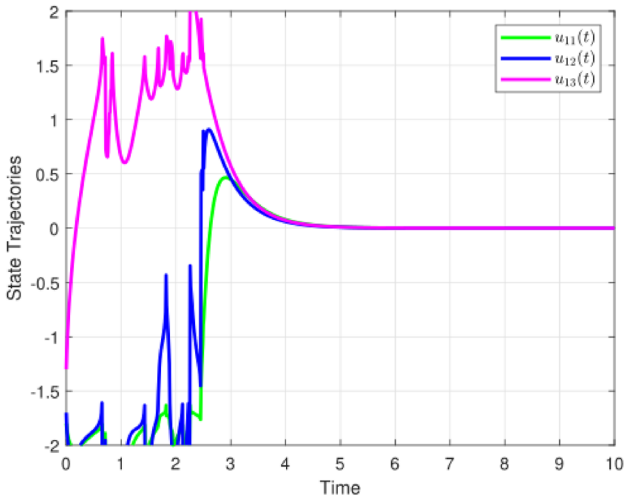

Fig. 3 State responses for $u_1(t)$ Example 1

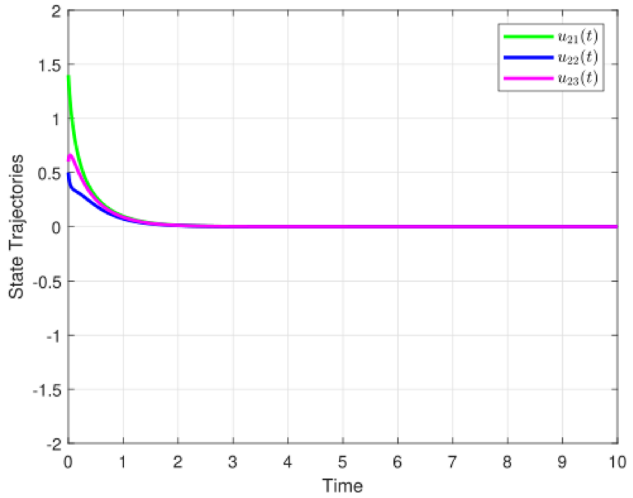

Fig. 4 State responses for $u_2(t)$ Example 1

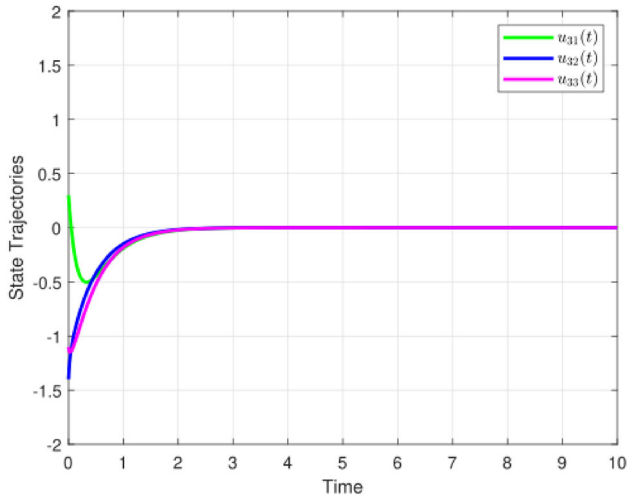

Fig. 5 State responses for $u_3(t)$ Example 1

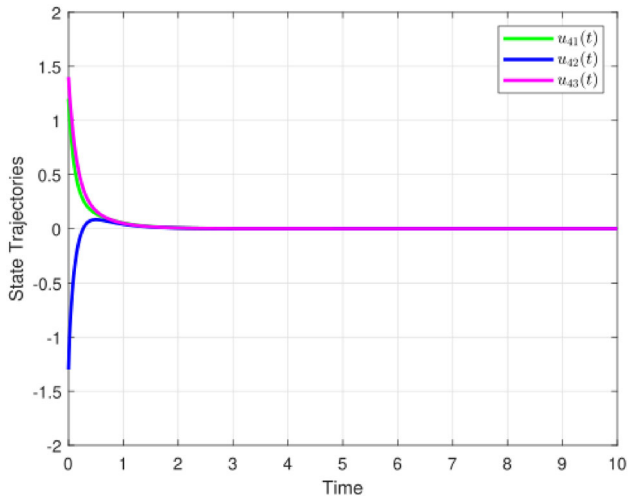

Fig. 6 State responses for $u_4(t)$ Example 1

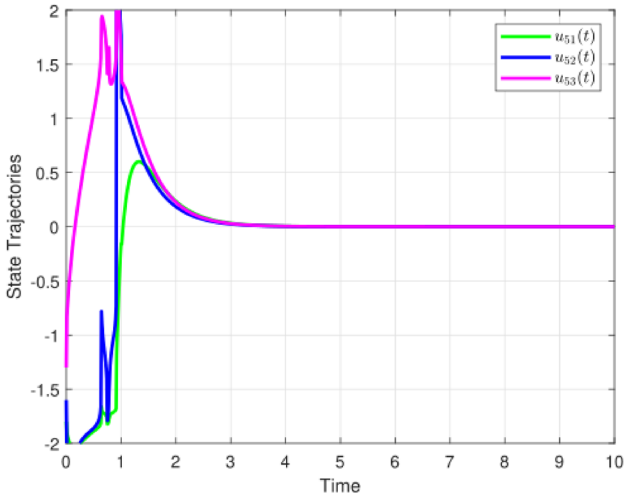

Fig. 7 State responses for $u_5(t)$ Example 1

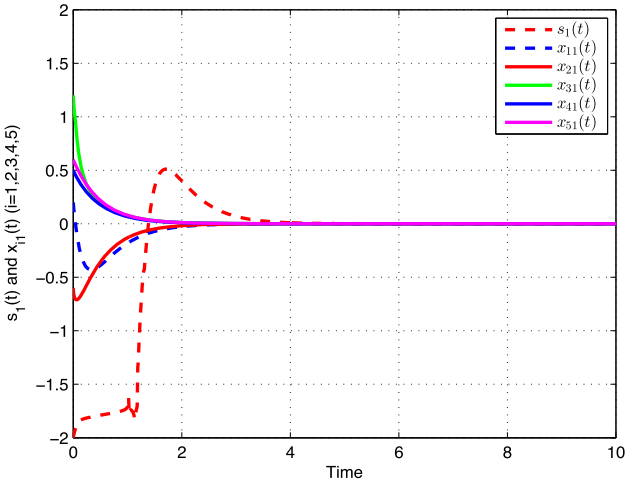

Fig. 8 State responses of $x_{i1}(t)$ $(i = 1, 2, 3, 4, 5)$ and $s_1(t)$ for Example 1

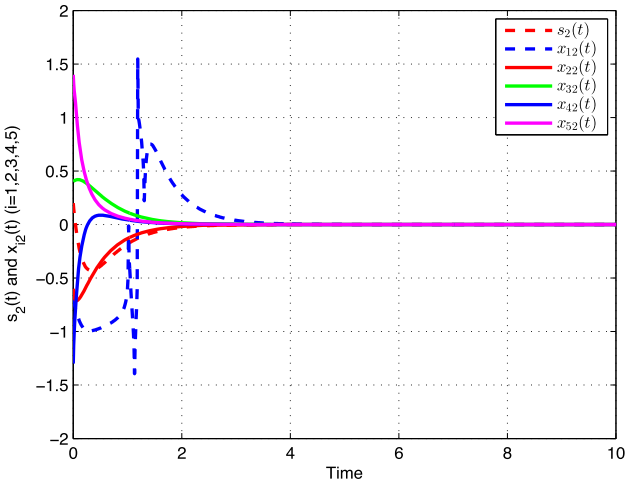

Fig. 9 State responses of $x_{i2}(t)$ $(i = 1, 2, 3, 4, 5)$ and $s_2(t)$ for Example 1

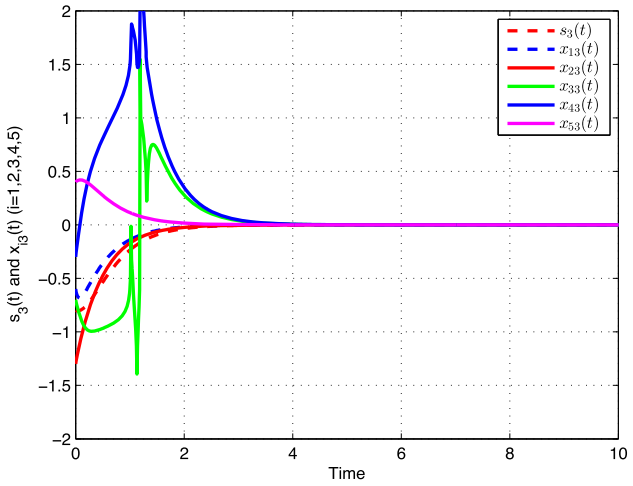

Fig. 10 State responses of $x_{i3}(t)$ $(i = 1, 2, 3, 4, 5)$ and $s_3(t)$ for Example 1

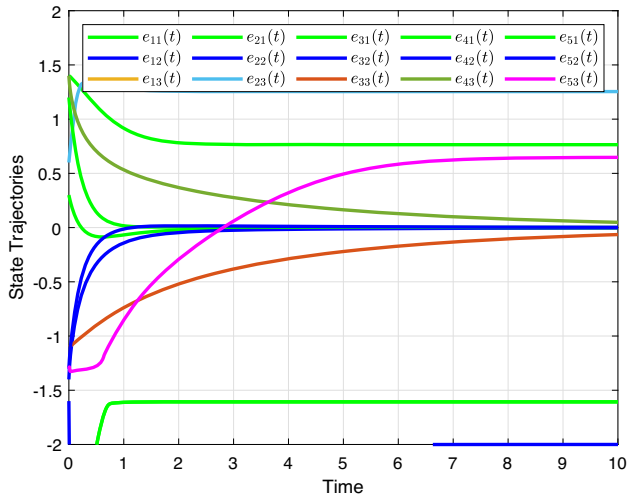

Fig. 11 State trajectories of system without control in Example 1

nization errors between the node states in Figs. 1 and 2 and the control inputs for all initial nodes in Figs. 3, 4, 5, 6, and 7. The system with the various state responses is simulated in Figs. 8, 9, and 10. Assume that the random initial values of the master system and the slave system in Figs. 8, 9, and 10 are initially the responses of the states $x_{i1}(t) - s_1(t)$, $x_{i2}(t) - s_2(t)$, $x_{i3}(t) - s_3(t)$ where $(i = 1, 2, 3, 4, 5)$. It can be clearly seen that the master and slave models are synchronized with the proposed control scheme. Therefore, the systems (1) and (2) can successfully synchronized. In addition, Fig. 11 shows the state responses without control inputs, while Fig. 12 shows the jump mode in Example 1. We have compared our results with different studies in Table 1, including [4,8,17,27,28], and discussed the advantages of this work. Overall, these results demonstrate the controller's ability to effectively synchronize the MJCDNs despite coupling delays.

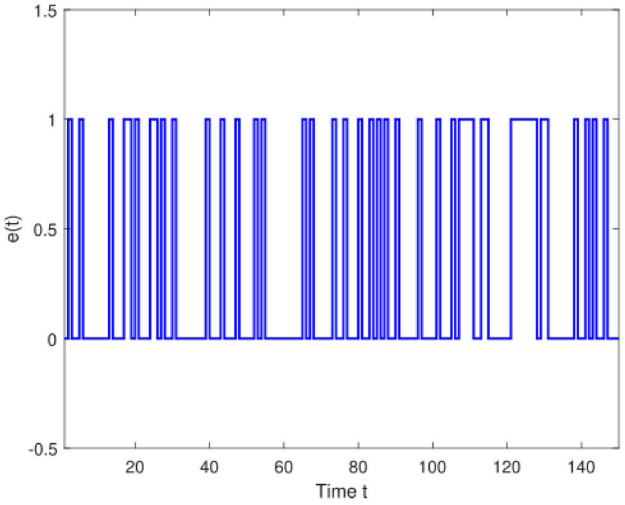

Fig. 12 Jumping modes responses in the Example 1

Table 1 Comparison with other works

Integer order	[4]	[8]	[28]	[17]	[27]	Our paper
CDNs	✓	✓	×	×	✓	✓
Fault-tolerant control	×	×	×	×	✓	✓
Markovian jump	×	×	✓	×	×	✓
T-S Fuzzy	×	×	✓	✓	×	✓
Synchronization	✓	✓	✓	×	✓	✓
MJCDNs	×	×	✓	×	×	✓

Example 2 In this example, we study the system (36) with a Markovian jump process where $p = 1, 2$, and apply it to a practical model. The Chua's oscillator is shown in Fig. 13. The model equations are given by [40,41]:

$$\begin{cases} \dot{x}_1(t) &= a_p\left(x_2(t) - m_p x_1(t) - g(x_1(t))\right) - b_p x_1(t-d(t)), \\ \dot{x}_2(t) &= x_1(t) - x_2(t) + x_3(t) - b_p x_1(t-d(t)), \\ \dot{x}_3(t) &= -c_p x_2(t) + b_p\left(2x_1(t-d(t)) - x_3(t-d(t))\right). \end{cases} \tag{37}$$

Here, $x_1(t)$, $x_2(t)$, and $x_3(t)$ represent the state variables of the oscillator. Parameters a_p, b_p, m_0, and m_p are con-

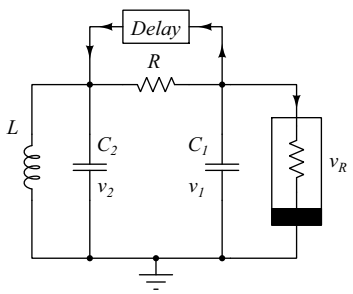

Fig. 13 Chua's oscillator for Example 2

stants defining the behavior of the oscillator. a_p is ratio of capacitances, m_0 nonlinear resistance parameter, m_p is linear resistance parameter, and b_p is parameter related to the resistance and capacitance. with the nonlinear characteristics

$$g(x(t)) = \frac{1}{2}\left(m_p - m_0)(|x_1(t)+1| - |x_1(t)-1|\right).$$

Let us consider a numerical example with the following parameter values: Let $a_1 = 10$, $b_1 = 14.87$, $a_2 = 9.5$, $b_2 = 13.65$, $c_1 = 0.1$, $c_2 = 0.09$, $m_0 = -1.27$, and $m_1 = m_2 = 0.68$.

Define $x(t) = [x_1(t), x_2(t), x_3(t)]$. Then, the known parameters can be expressed as the following matrix equation:

$$R_1 = \begin{bmatrix} -a_1 m_1 & a_1 & 0 \\ 1 & -1 & 1 \\ 0 & -b_1 & 0 \end{bmatrix}, \quad R_2 = \begin{bmatrix} -a_2 m_2 & a_2 & 0 \\ 1 & -1 & 1 \\ 0 & -b_2 & 0 \end{bmatrix},$$

$$C_1 = \begin{bmatrix} a_1(m_1 - m_0) & 0 & 0 \\ 0 & 0 & 0 \\ 0 & 0 & 0 \end{bmatrix}, \quad C_2 = \begin{bmatrix} a_2(m_2 - m_0) & 0 & 0 \\ 0 & 0 & 0 \\ 0 & 0 & 0 \end{bmatrix},$$

$$\tilde{\Lambda}_1 = \begin{bmatrix} -c_1 & 0 & 0 \\ -c_1 & 0 & 0 \\ 2c_1 & 0 & -c_1 \end{bmatrix}, \quad \tilde{\Lambda}_2 = \begin{bmatrix} -c_2 & 0 & 0 \\ -c_2 & 0 & 0 \\ 2c_2 & 0 & -c_2 \end{bmatrix}$$

The other parameter matrix is given as follows:

$$W_1 = W_2 = \begin{bmatrix} -2.1 & 1.2 & 0.1 \\ 0 & -2.2 & 0.1 \\ 0 & 1 & -3.3 \end{bmatrix},$$

$$\mathfrak{F}_{01} = \mathfrak{F}_{02} = diag\{0.3,\ 0.35,\ 0.4,\ 0.44,\ 0.51,\ 0.55,\ 0.16,\ 0.56,\ 0.48,\ 0.52,\ 0.77,\ 0.78\},$$

and the outer coupling matrices are

$$\tilde{D}_1 = \tilde{D}_2 = \begin{bmatrix} -1.5 & 0.2 & 0.2 & 1.3 \\ 0 & 1.2 & 3.1 & 0 \\ 0 & 0.4 & -0.4 & 0.2 \\ 1.4 & 0 & -0.2 & 0.6 \end{bmatrix}.$$

We can obtain that the gain matrix as follows:

$$K_1 = diag\{K_{11}, K_{12}, K_{13}, K_{14}\},$$
$$K_2 = diag\{K_{21}, K_{22}, K_{23}, K_{24}\},$$

$$K_{11} = \begin{bmatrix} -0.4251 & 0.0589 & -0.5267 \\ -0.0378 & -0.5243 & -0.1353 \\ -0.0341 & -0.3630 & -0.1310 \end{bmatrix},$$

$$K_{12} = \begin{bmatrix} -0.3301 & 0.0599 & -0.3699 \\ -0.0239 & -0.4167 & -0.0891 \\ -0.0231 & -0.3082 & -0.0929 \end{bmatrix},$$

$$K_{13} = \begin{bmatrix} -0.5574 & 0.4459 & -1.1721 \\ -0.0432 & -0.0140 & -0.1306 \\ -0.0519 & 0.0202 & -0.1952 \end{bmatrix},$$

$$K_{14} = \begin{bmatrix} -0.2804 & 0.1361 & -0.3609 \\ -0.0266 & -0.1902 & -0.0710 \\ -0.0245 & -0.1450 & -0.0781 \end{bmatrix},$$

$$K_{21} = \begin{bmatrix} -4.0582 & 4.0438 & -4.4480 \\ -0.0225 & -0.2568 & -0.0668 \\ -0.0395 & -0.1096 & -0.1744 \end{bmatrix},$$

$$K_{22} = \begin{bmatrix} -3.1895 & 3.3497 & -3.1724 \\ -0.0160 & -0.1979 & -0.0483 \\ -0.0283 & -0.0983 & -0.1291 \end{bmatrix},$$

$$K_{23} = \begin{bmatrix} -4.8411 & 5.1550 & -9.3277 \\ -0.0244 & 0.0046 & -0.0721 \\ -0.0616 & 0.1325 & -0.3403 \end{bmatrix},$$

$$K_{24} = \begin{bmatrix} -2.6508 & 3.1046 & -3.1413 \\ -0.0175 & -0.0805 & -0.0435 \\ -0.0222 & -0.0265 & -0.1086 \end{bmatrix}.$$

We will solve the system numerically and plot the trajectories of the oscillator's states. The Chua oscillator exhibits complex dynamical behavior, including chaotic oscillations. Figure 14 graphically indicates the chaotic behavior of Chua's circuit. It has been extensively studied in the field of nonlinear dynamics and chaos theory. The oscillator's behavior is highly sensitive to its parameters, and it can display a wide range of phenomena, including attractors with fractal structure. Employing this approach, we examined and analyzed synchronization in this specific case. We successfully addressed the LMI described in Theorem 2 for

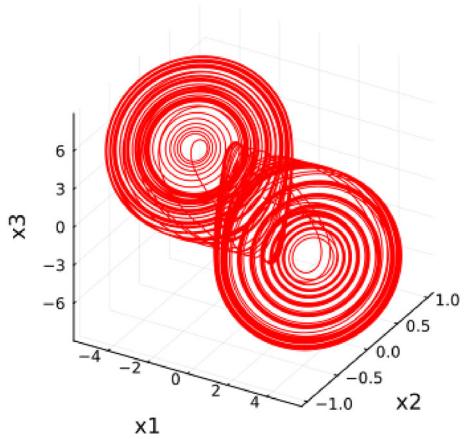

Fig. 14 Chaotic behavior of the Chua's circuit described in Example 2

the system (36). The results of the numerical simulation are shown in Figs. 15, 16, 17, 18, 19, and 20. Figures 15 and 16 show the state responses of the fault-tolerant control system. Figures 17, 18, 19 and 20 show the input control for each node individually. The system with the various state responses is simulated in Figs. 21, 22, and 23. Assume that the random initial values of the master system and the slave system in Figs. 21, 22, and 23 are initially the responses of the states $x_{i1}(t) - s_1(t), x_{i2}(t) - s_2(t), x_{i3}(t) - s_3(t)$ where $(i = 1, 2, 3, 4)$. It can be clearly seen that the master and slave models are synchronized with the proposed control scheme. Therefore, the systems (1) and (2) can successfully synchronized. Analysis of Figs. 15, 16, 17, 18, 19, and 20 suggests that the T-S fuzzy CDNs governed by (11) display mean-square stability. This observation emphasizes the robustness and effectiveness of the proposed method in maintaining stability and fault tolerance in complex networked

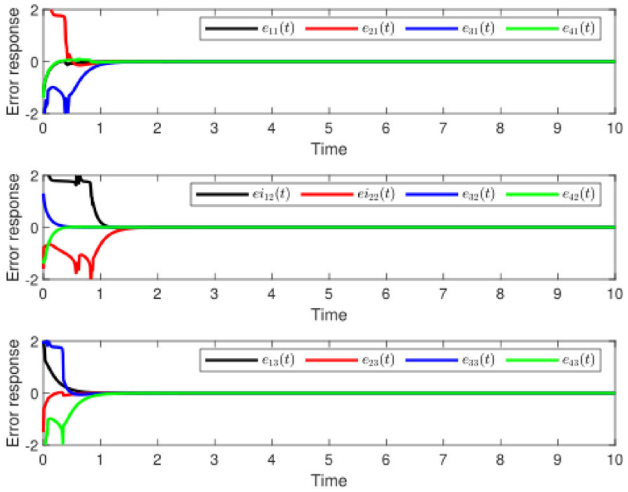

Fig. 15 State responses for the error system for Example 2

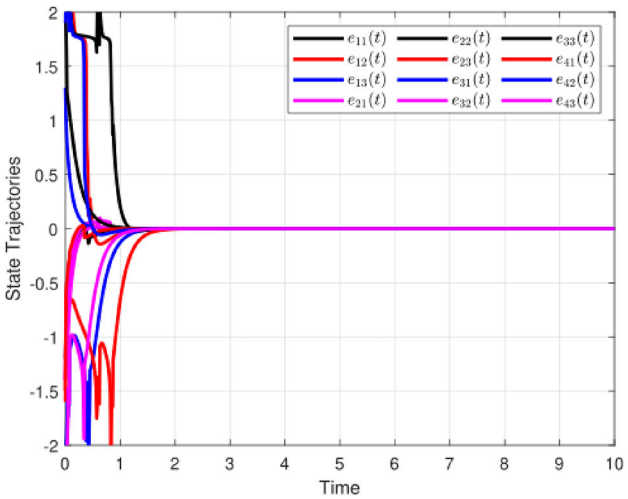

Fig. 16 State responses for the error system for Example 2

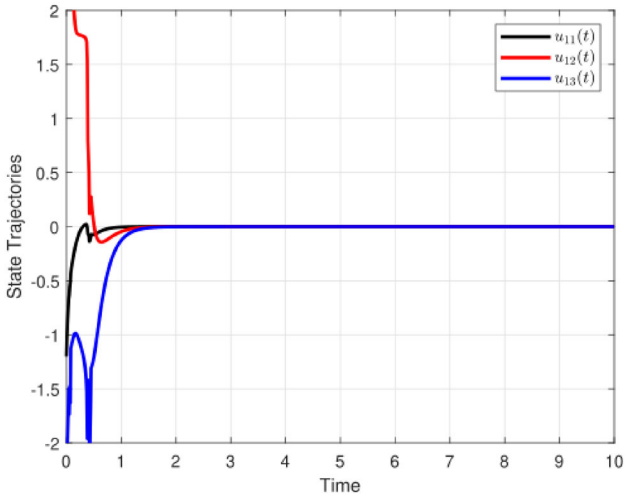

Fig. 17 Response of control input $u_1(t)$

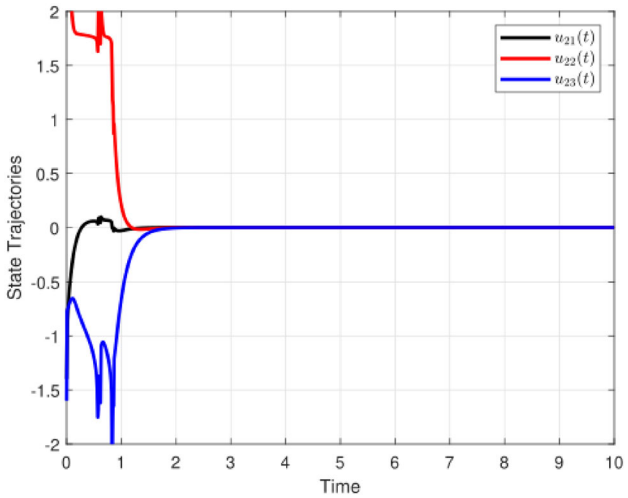

Fig. 18 Response of control input $u_2(t)$

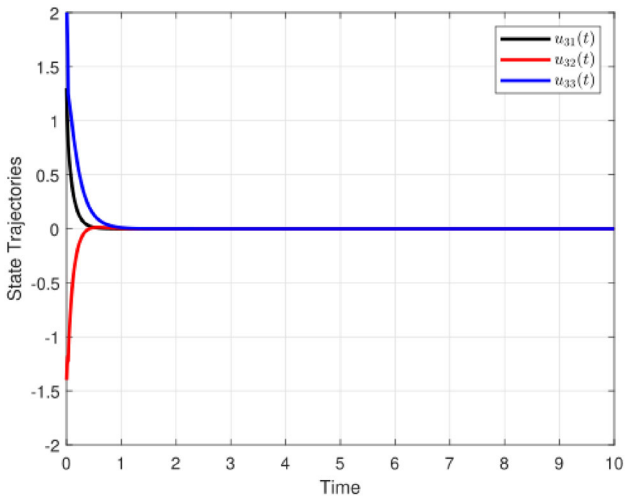

Fig. 19 Response of control input $u_3(t)$

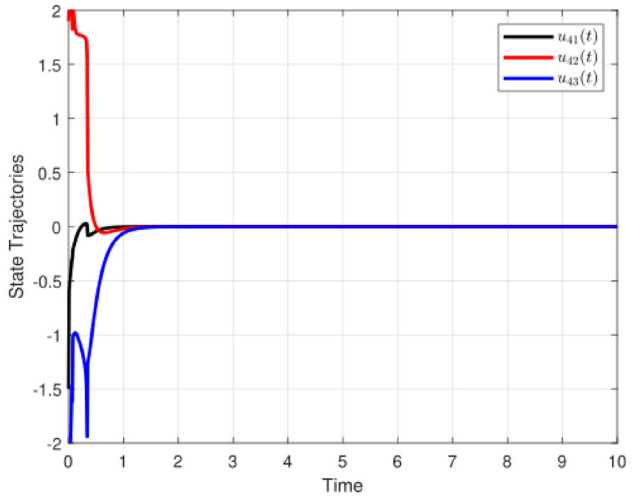

Fig. 20 Response of control input $u_4(t)$

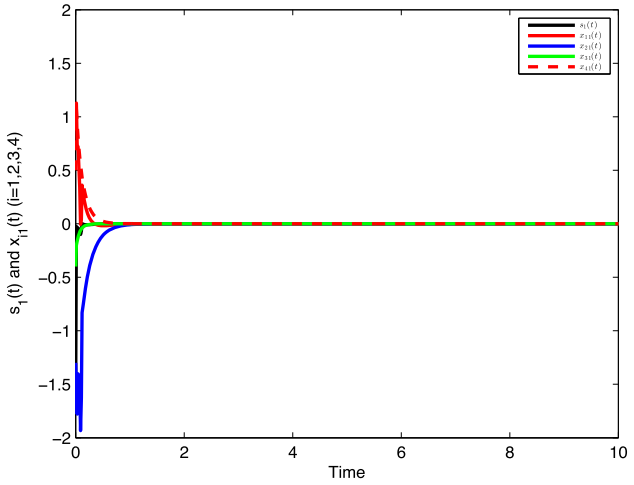

Fig. 21 State responses of $x_{i1}(t)$ $(i = 1, 2, 3, 4)$ and $s_1(t)$ for Example 2

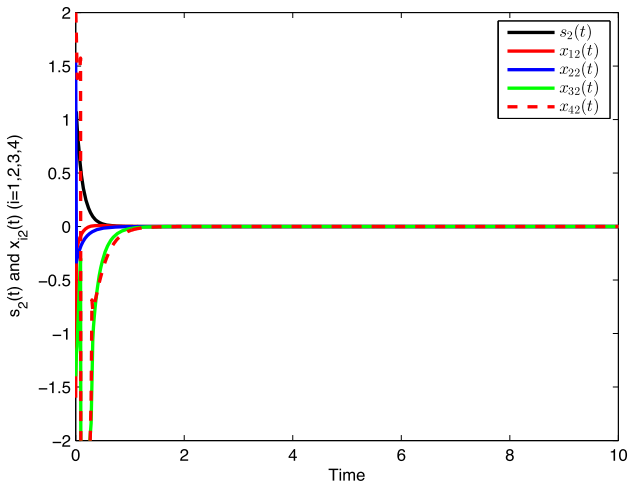

Fig. 22 State responses of $x_{i1}(t)$ $(i = 1, 2, 3, 4)$ and $s_2(t)$ for Example 2

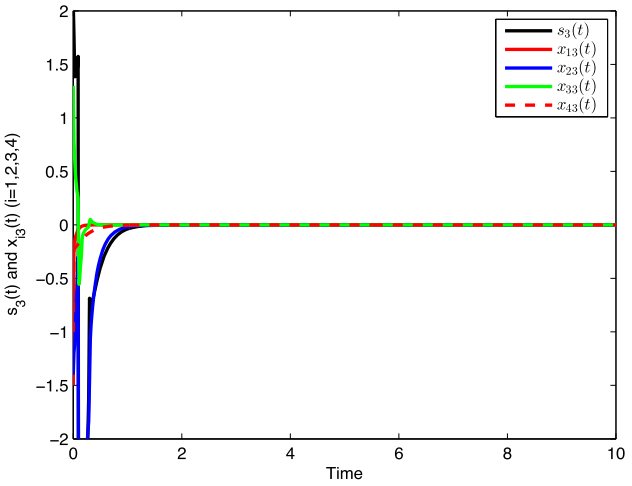

Fig. 23 State responses of $x_{i1}(t)$ $(i = 1, 2, 3, 4)$ and $s_3(t)$ for Example 2

systems. Moreover, the results provide valuable insights into the dynamics and control mechanisms of such networks under different conditions, thus contributing to the advancement of control theory and practice.

Remark 5 Synchronization approach with fault-tolerant control, T-S fuzzy, and Markovian jumping difficulties are not usually employed for complex dynamical networks. Some scientific publications have addressed such issues. However, the authors used usual LKFs and simple examples to solve the stability problems in those articles. A novel LKF with the information of coupling delay, fuzzy rules, Markov modes, and some integral inequalities is proposed for the stability analysis of fault-tolerant control with synchronization approach in this paper, considering that some computational complexity can occur in our method. However, fault-tolerant control with T-S fuzzy Markovian jumping problem was completely studied for CDNs with mixed time delays, which is the main contribution and motivation of our work.

Remark 6 In this study, we will deduce the system and applied the proposed method to a similar system as in [42], aiming to evaluate and compare the maximum allowable upper bound (MAUB) of time-varying delays. Also, we have taken the same parameter values from [42]. The MAUB results presented in Table 2 demonstrate that our approach consistently achieves higher values across different parameters ($\lambda = 0.8, 0.9,$ and 1.0), with our method yielding

Table 2 MAUB α for different values of λ

λ	0.8	0.9	1.0
[42]	4.1089	2.7983	2.3562
Our result	6.0978	5.8098	4.0652

MAUBs. The results significantly surpass those reported in [42]. This demonstrates that our approach not only increases the MAUB of time-varying delays but also enhances the convergence speed of the system, making it more effective and efficient in practical applications. This comparison highlights the superior performance and robustness of the proposed method in handling time-varying delays within complex dynamical networks.

5 Conclusion

This paper investigates master–slave synchronization in MJCDNs using T-S fuzzy model techniques. It focuses on fault-tolerant control mechanisms and control gain matrices for efficient system regulation. Stability analysis is conducted using Lyapunov functions, leading to the formulation of constraints as LMIs. The proposed controller is validated using MATLAB's LMI toolbox, proving its suitability for complex networks with large nodes due to low installation costs and reduced time requirements. Future research will explore adaptive fault-tolerant methods for sampled data systems. Simulation results demonstrate the validity of the main results.

Author contributions Conceptualization: Saravanan Shanmugam, and R. Vadivel; methodology: Saravanan Shanmugam, Mohamed Rhaima, and G. Brundhashree; formal analysis: S. Magudeeswaran and Nallappan Gunasekaran; investigation: R. Vadivel and Nallappan Gunasekaran; writing—original draft: Saravanan Shanmugam and G. Brundhashree; writing—review & editing: G. Brundhashree, Mohamed Rhaima, and S. Magudeeswaran; and supervision: R. Vadivel and Nallappan Gunasekaran.

Funding M. Rhaima was supported by Researchers Supporting Project number (RSPD2024R683) King Saud University, Riyadh, Saudi Arabia.

Data availability Not applicable.

Declarations

Conflict of interest The author declares that there is no conflict of interest regarding the publication of this paper.

Ethical Approval Not applicable.

References

1. Feng, J., Yang, P., Zhao, Y.: Cluster synchronization for nonlinearly time-varying delayed coupling complex networks with stochastic perturbation via periodically intermittent pinning control. Appl. Math. Comput. **291**, 52–68 (2016)
2. Guo, J., Wang, Y., Bo, Y.: Almost sure finite-time synchronization of Markov jump complex dynamical networks with asynchronous switching. Neurocomputing **574**, 127275 (2024)
3. Feng, J., Cheng, K., Wang, J., Deng, J., Zhao, Y.: Pinning synchronization for delayed coupling complex dynamical networks with incomplete transition rates Markovian jump. Neurocomputing **434**, 239–248 (2021)
4. Yu, T., Cao, D., Yang, Y., Liu, S., Huang, W.: Robust synchronization of impulsively coupled complex dynamical network with delayed nonidentical nodes. Chaos Solitons Fractals **87**, 92–101 (2016)
5. Fang, M.: Synchronization for complex dynamical networks with time delay and discrete-time information. Appl. Math. Comput. **258**, 1–11 (2015)
6. Liu, L., Wang, Y., Gao, Z.: Tracking control for the dynamic links of discrete-time complex dynamical network via state observer. Appl. Math. Comput. **369**, 124857 (2020)
7. Gao, P., Wang, Y., Zhao, J., Zhang, L., Peng, Y.: Links synchronization control for the complex dynamical network. Neurocomputing **515**, 59–67 (2023)
8. Su, L., Fan, C.: Static output feedback synchronization for Markov jump complex dynamical networks with time-varying delay. J. Frankl. Inst. **361**, 106684 (2024)
9. Hu, Z., Ren, H., Shi, P.: Synchronization of complex dynamical networks subject to noisy sampling interval and packet loss. IEEE Trans. Neural Netw. Learn. Syst. **33**(8), 3216–3226 (2021)
10. Ali, M.S., Saravanan, S., Cao, J.: Finite-time boundedness, l2-gain analysis and control of Markovian jump switched neural networks with additive time-varying delays. Nonlinear Anal.: Hybrid Syst. **23**, 27–43 (2017)
11. Li, J., Shen, L., Yao, F., Zhao, H., Wang, J.: An event-triggered approach to finite-time observer-based control for Markov jump systems with repeated scalar nonlinearities. Trans. Inst. Meas. Control **40**(9), 2789–2797 (2018)
12. Shu, Y., Liu, X.-G., Qiu, S., Wang, F.: Dissipativity analysis for generalized neural networks with Markovian jump parameters and time-varying delay. Nonlinear Dyn. **89**, 2125–2140 (2017)
13. Shen, H., Zhu, Y., Zhang, L., Park, J.H.: Extended dissipative state estimation for Markov jump neural networks with unreliable links. IEEE Trans. Neural Netw. Learn. Syst. **28**(2), 346–358 (2016)
14. He, Q., Ma, Y.: Non-fragile sliding mode control for H_∞/passive synchronization of Master-slave Markovian jump complex dynamical networks with time-varying delays. Neural Comput. Appl. **34**(3), 2323–2340 (2022)
15. Selvaraj, P., Sakthivel, R., Ahn, C.K.: Observer-based synchronization of complex dynamical networks under actuator saturation and probabilistic faults. IEEE Trans. Syst. Man Cybern.: Syst. **49**(7), 1516–1526 (2018)
16. Suresh, R., Saravanan, S., Dutta, H., Vadivel, R., Gunasekaran, N.: Extended dissipativity-based sampled-data controller design for fuzzy distributed parameter systems. Math. Found. Comput. (2024). https://doi.org/10.3934/mfc.2024006
17. Shanmugam, S., Hong, K.-S.: An Event-triggered extended dissipative control for Takagi-Sugeno fuzzy systems with time-varying delay via free-matrix-based integral inequality. J. Frankl. Inst. **357**(12), 7696–7717 (2020)
18. Kwon, O., Park, M.-J., Park, J.H., Lee, S.-M.: Stability and stabilization of T-S fuzzy systems with time-varying delays via augmented Lyapunov-Krasovskii functionals. Inf. Sci. **372**, 1–15 (2016)
19. Wang, T., Zhao, F., Chen, X., Qiu, J.: A novel preassigned-time sliding mode control method for synchronization of T-S fuzzy stochastic complex networks with time-varying delay. Asian J. Control (2024). https://doi.org/10.1002/asjc.3368
20. Zheng, W., Wang, H., Wang, H., Zhang, Z.: Dynamic output feedback control with output quantizer for nonlinear uncertain T-S fuzzy systems with multiple time-varying input delays and unmatched disturbances. Asian J. Control **22**(5), 1901–1918 (2020)

21. Fu, H., Zhou, C., Ma, C.: Dual asynchronous control for T-S fuzzy semi-Markov jump systems: a finite-time design. Asian J. Control **26**(1), 137–149 (2024)
22. Sakthivel, R., Sakthivel, R., Kwon, O.-M., Selvaraj, P.: Synchronisation of stochastic T-S fuzzy multi-weighted complex dynamical networks with actuator fault and input saturation. IET Control Theory Appl. **14**(14), 1957–1967 (2020)
23. Qin, C., Lin, W.-J.: Adaptive event-triggered fault-tolerant control for Markov jump nonlinear systems with time-varying delays and multiple faults. Commun. Nonlinear Sci. Numer. Simul. **128**, 107655 (2024)
24. Habibzadeh, H., Ziaei, A., Kharrati, H., Rahimi, A.: Fault-tolerant consensus control for Hybrid Multi-agent systems. In: 2022 IEEE International Conference on Prognostics and Health Management (ICPHM), pp. 64–69. IEEE (2022)
25. Chen, W., Hu, Q.: Sliding-mode-based attitude tracking control of spacecraft under reaction wheel uncertainties. IEEE/CAA J. Autom. Sin. (2022). https://doi.org/10.1109/JAS.2022.105665
26. Zhang, C., Dai, M.-Z., Wu, J., Xiao, B., Li, B., Wang, M.: Neural-networks and Event-based fault-tolerant control for spacecraft attitude stabilization. Aerosp. Sci. Technol. **114**, 106746 (2021)
27. Ye, D., Yang, X., Su, L.: Fault-tolerant synchronization control for complex dynamical networks with semi-Markov jump topology. Appl. Math. Comput. **312**, 36–48 (2017)
28. Divya, H., Sakthivel, R., Liu, Y.: Delay-dependent synchronization of T-S fuzzy Markovian jump complex dynamical networks. Fuzzy Sets Syst. **416**, 108–124 (2021)
29. Zhong, Y., Song, D.: Nonfragile synchronization control of T-S fuzzy Markovian jump complex dynamical networks. Chaos Solitons Fractals **170**, 113342 (2023)
30. Tomescu, M.-L., Preitl, S., Precup, R.-E., Tar, J.K.: Stability analysis method for fuzzy control systems dedicated controlling nonlinear processes. Acta Polytech. Hung. **4**(3), 127–141 (2007)
31. Ku, C.-C., Chang, W.-J., Huang, Y.-M.: Robust observer-based fuzzy control via proportional derivative feedback method for singular Takagi-Sugeno fuzzy systems. Int. J. Fuzzy Syst. **24**(8), 3349–3365 (2022)
32. Precup, R.-E., Preitl, S., Petriu, E., Bojan-Dragos, C.-A., Szedlak-Stinean, A.-I., Roman, R.-C., Hedrea, E.-L.: Model-based fuzzy control results for networked control systems. Rep. Mech. Eng. **1**(1), 10–25 (2020)
33. Precup, R.-E., Nguyen, A.-T., Blažič, S.: A survey on fuzzy control for mechatronics applications. Int. J. Syst. Sci. **55**(4), 771–813 (2024)
34. Wang, J., Shen, H.: Passivity-based fault-tolerant synchronization control of chaotic neural networks against actuator faults using the semi-Markov jump model approach. Neurocomputing **143**, 51–56 (2014)
35. Wang, J., Park, J.H., Shen, H.: New delay-dependent bounded real lemmas of polytopic uncertain singular Markov jump systems with time delays. J. Frank. Inst. **351**(3), 1673–1690 (2014)
36. Wang, Z., Liu, Y., Liu, X.: H_∞ filtering for uncertain stochastic time-delay systems with sector-bounded nonlinearities. Automatica **44**(5), 1268–1277 (2008)
37. Park, P., Lee, W.I., Lee, S.Y.: Auxiliary function-based integral inequalities for quadratic functions and their applications to time-delay systems. J. Frankl. Inst. **352**(4), 1378–1396 (2015)
38. Seuret, A., Gouaisbaut, F.: Wirtinger-based integral inequality: application to time-delay systems. Automatica **49**(9), 2860–2866 (2013)
39. Park, M., Kwon, O., Park, J.H., Lee, S., Cha, E.: Stability of time-delay systems via Wirtinger-based double integral inequality. Automatica **55**, 204–208 (2015)
40. Rakkiyappan, R., Latha, V.P., Sivaranjani, K.: Exponential H_∞ synchronization of Lur'e complex dynamical networks using pinning sampled-data control. Circuits Syst. Signal Process. **36**(10), 3958–3982 (2017)
41. Wang, J., Su, L., Shen, H., Wu, Z.-G., Park, J.H.: Mixed H_∞/passive sampled-data synchronization control of complex dynamical networks with distributed coupling delay. J. Frankl. Inst. **354**(3), 1302–1320 (2017)
42. Huang, X., Ma, Y.: Finite-time H_∞ sampled-data synchronization for Markovian jump complex networks with time-varying delays. Neurocomputing **296**, 82–99 (2018)

G. Brundhashree was born in 1998. She obtained her Bachelor's degree in Mathematics from Gobi Arts & Science College, Gobichettipalayam, affiliated with Bharathiar University, Tamil Nadu, India, in 2018. She then completed her Master's degree in Mathematics from Dr. N.G.P. Arts and Science College, Bharathiar University, Coimbatore, Tamil Nadu, in 2020. Her current research interests focus on finite-time control of time-delay systems, stochastic stability, nonlinear systems, Markovian jump systems, fuzzy systems, and multi-agent systems.

Saravanan Shanmugam was born in 1990. He received the Bachelor's degree from the Department of Mathematics, Government Arts University, Thiruvannamalai, Thiruvalluvar University, Vellore, Tamil Nadu, India, in 2011, the Master's degree in Mathematics from Madras Christian University, University of Madras, Chennai, Tamil Nadu, in 2013, and the Doctor of Philosophy degree in Mathematics from Thiruvalluvar University in 2018. From January 2018 to July 2018, he was a Visiting Research Fellow at the Department of Industrial Engineering, Pusan National University, Busan, South Korea. He was a PNU Post-doctoral Research Fellow at the School of Mechanical Engineering, Pusan National University. He was a Research facult at the Centre for Nonlinear Systems, Chennai Institute of Technology, Chennai, India, from Nov 2022 to Sep 2024. He is currently working at the Center for Computational Biology, Easwari Engineering College, Chennai, India. His current research interests include finite-time control of time-delayed systems, stochastic stability, nonlinear systems, Markovian jump systems, H∞ control, and multi-agent systems. He is a reviewer for several SCI journals.

S. Magudeeswaran was born in 1995. He received both his Bachelor's and Master's degrees in Mathematics from the Sri Ramakrishna Mission Vidyalaya College of Arts and Science, Coimbatore, affiliated with Bharathiar University, Tamil Nadu, India, in 2015 and 2017, respectively. He earned his M.Phil and Doctor of Philosophy (Ph.D.) in Mathematics from the same institution in 2019 and 2022 respectively. Currently, he is working as an Assistant professor at Sree Saraswathi Thyagaraja College, Pollachi, India. His research interests include Differential Equations, Mathematical Biology, and Nonlinear Dynamics. He also serves as a reviewer for various international journals, including the International Journal of Current Science, the International Journal of Creative Research and Thoughts, the International Journal of Advanced Research and Development, and the Journal of Applied Science and Engineering.

R. Vadivel received his B. Sc., M.Sc., M.Phil. Degrees in Mathematics from Sri Ramakrishna Mission Vidyalaya College of Arts and Science affiliated to Bharathiar University, Tamil Nadu, India, and Ph.D. in Mathematics from the Department of Mathematics, Thiruvalluvar University, India. He was a post-doctoral research fellow at the Research Center for Wind Energy Systems, Kunsan National University, Gunsan, South Korea, from 2018 to 2019. Currently, he is working as a lecturer in the Department of Mathematics, Faculty of Science and Technology, Phuket Rajabhat University, Thailand. He has authored and co-authored more than 60 research articles in various SCI journals. His research interests include control theory, stability analysis, event-triggered control, networked control systems, neural networks, and T-S fuzzy theory. He serves as a reviewer for various SCI journals.

Nallappan Gunasekaran received the PhD Degree in Mathematics/ from Thiruvalluvar University, Vellore, India, in 2018. He was a Junior Research Fellow with the Department of Science and Technology-Science and Engineering Research Board (DST-SERB), Government of India, New Delhi, India. He was a Post-doctoral Research Fellow in the Research Center for Wind Energy Systems, Kunsan National University, Gunsan, South Korea, from 2017 to 2018. He was a Post-doctoral Research Fellow in Department of Mathematical Sciences, Shibaura Institute of Technology, Saitama, Japan, from 2018 to 2020. He was a Post-doctoral Research Fellow in Computational Intelligence Laboratory, Toyota Technological Institute, Japan. Currently, he is working as an Associate professor in Eastern Michigan Joint College of Engineering, Beibu Gulf University, Qinzhou, 535011, China. His research interests are deep learning, natural language processing, complex dynamical networks, cryptography, etc. He serves as a Reviewer for various SCI journals. He has authored and co-authored more than 100 research articles in various SCI journals.

Mohamed Rhaima was born in 1984. He received the M.Sc. degree in mathematics from the Faculty of Sciences of Tunis, Tunisia, in 2012, and the Ph.D. degree in mathematics from the University of Tunis El Manar, Tunisia, and Tor Vergata University, Rome, Italy, in 2017. His research interests include nonlinear stochastic control systems, nonlinear stochastic dynamical systems, stochastic fractional-order systems, and stochastic delay systems.